

DTIC FILE COPY

(U)

SECURITY CLASSIFICATION OF THIS PAGE

Form Approved
OMB No 0704-0188

REPORT DOCUMENTATION PAGE

| | | |
|---|--|--|
| 1. | 1b RESTRICTIVE MARKING NA | |
| 2. | 3 DISTRIBUTION/AVAILABILITY OF REPORT Distribution Unlimited | |
| 2 | 5 MONITORING ORGANIZATION REPORT NUMBER(S) Office of Naval Research | |
| 4 | 6a NAME OF PERFORMING ORGANIZATION American Red Cross 6b OFFICE SYMBOL (If applicable) NA | |
| | 7a NAME OF MONITORING ORGANIZATION Office of Naval Research | |
| | 6c ADDRESS (City, State, and ZIP Code) 20855 Jerome H. Holland Laboratory 15601 Crabb's Branch Way, Rockville, MD | |
| | 7b ADDRESS (City, State, and ZIP Code) 800 N. Quincy St Arlington, VA 22217-5000 | |
| | 8a. NAME OF FUNDING / SPONSORING ORGANIZATION Office of Naval Research 8b OFFICE SYMBOL (If applicable) ONR | |
| | 9 PROCUREMENT INSTRUMENT IDENTIFICATION NUMBER N00014 - 90 - J - 1562 | |
| | 8c. ADDRESS (City, State, and ZIP Code) 800 N. Quincy Street Arlington, VA 22217-5000 | |
| | 10 SOURCE OF FUNDING NUMBERS PROGRAM ELEMENT NO 61153N PROJECT NO RR04108 TASK NO 4414022---01 WORK UNIT ACCESSION NO | |
| 11 TITLE (Include Security Classification) Workshop on Biophysics of Transmembrane Electric Fields (U) | | |
| 12 PERSONAL AUTHOR(S) Arthur E. Sowers | | |
| 13a. TYPE OF REPORT Proceedings | 13b TIME COVERED FROM 01JAN90 TO 31DEC90 | 14 DATE OF REPORT (Year, Month, Day) NOV 15, 1990 |
| 15 PAGE COUNT 92 | | |
| 16 SUPPLEMENTARY NOTATION See notice of grant award signed by Mary Ann Cook dated Feb 1, 1990 | | |
| 17 COSATI CODES FIELD 08 | 18 SUBJECT TERMS (Continue on reverse if necessary and identify by block number) Membrane, Biophysics, Electric Fields, Sensing, Ion Channels, Voltage | |
| 19 ABSTRACT (Continue on reverse if necessary and identify by block number) Proceedings includes abstracts submitted by invited speakers | | |
| DTIC ELECTED MAR 13 1991 S E D | | <div style="border: 1px solid black; padding: 2px; margin-bottom: 5px;">DISTRIBUTION STATEMENT A</div> <div style="border: 1px solid black; padding: 2px; display: inline-block;">Approved for public release Distribution unlimited</div> |
| 20 DISTRIBUTION/AVAILABILITY OF ABSTRACT <input checked="" type="checkbox"/> UNCLASSIFIED/UNLIMITED <input type="checkbox"/> SAME AS RPT <input type="checkbox"/> DTIC USERS | | 21 ABSTRACT SECURITY CLASSIFICATION (U) |
| 22a NAME OF RESPONSIBLE INDIVIDUAL Dr. Igor Vodyanov | | 22b TELEPHONE (Include Area Code) 703-696-4056 22c OFFICE SYMBOL ONR |

**INTERNATIONAL CONFERENCE
ON THE
BIOPHYSICS OF TRANSMEMBRANE ELECTRIC FIELDS**

October 23 - October 26

1990

at the

Belmont House

Elkridge, Maryland

Organizer:

Arthur E. Sowers

Co-organizers:

**Yu. Chizmadzhev
A. Parsegian
I. Vodyanoy**

Sponsors:

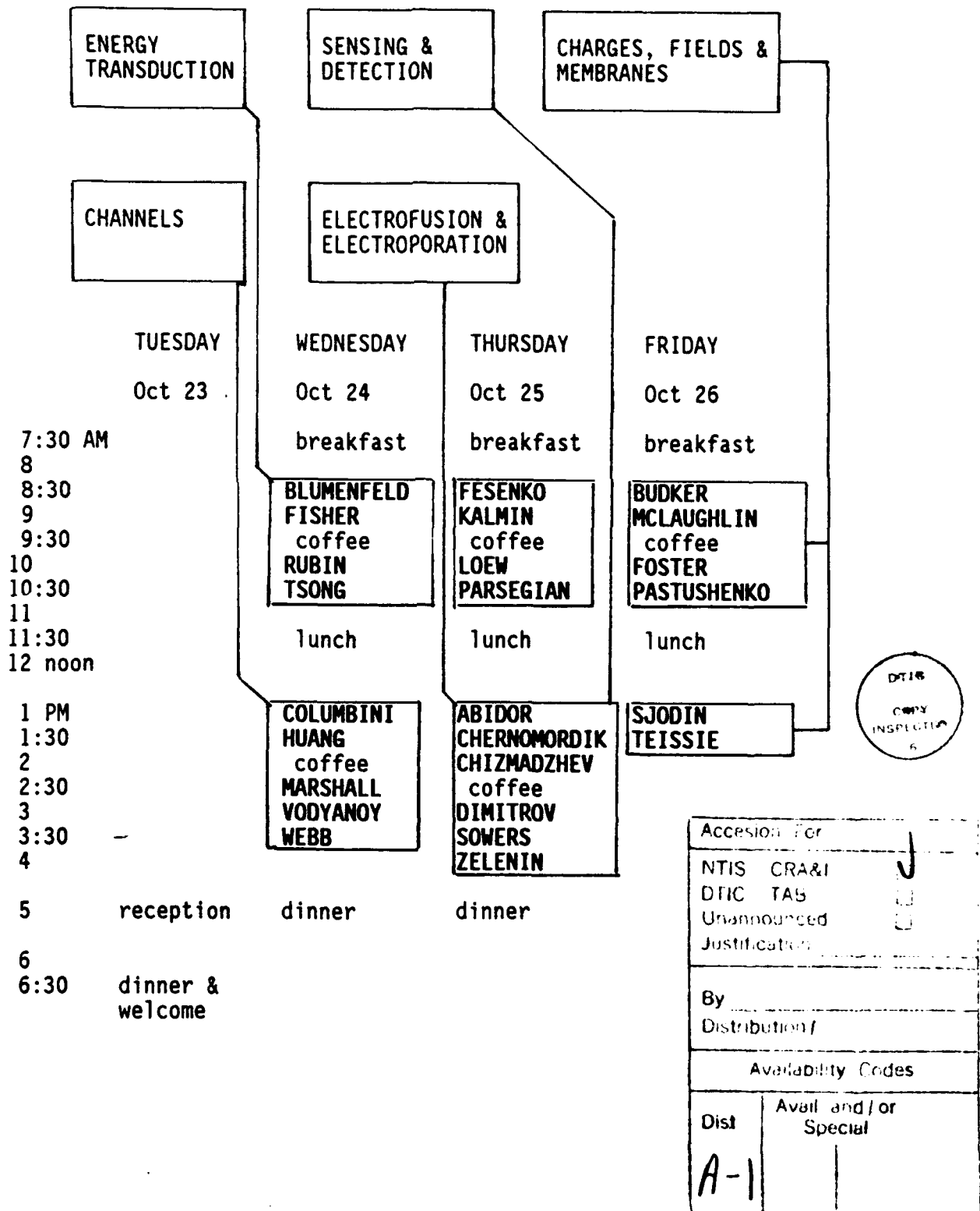
**American National Red Cross
Office of Naval Research
Electric Power Research Institute
Costar Corporation
Gibco BRL**

~~00 11 1 03 17~~

91 3 13 029

FINAL PROGRAM

International Conference on the Biophysics of Transmembrane Electric Fields



CONFERENCE PROGRAM

Session Titles, Names, and Titles of presentations

WEDNESDAY, OCTOBER 24

Energy Transduction

- 8:30 AM BLUMENFELD: Physics of ATP formation in the energy-transducing membranes of mitochondria and chloroplasts
- 9:00 FISHER: The transduction of protein-ligand binding energy into driving forces for catalytic, mechanical, conformationsl, and other forms of biological work
- 9:30 (coffee)
- 10:00 RUBIN: Conformational dynamics and electron transfer (E_t) in photosynthetic membrane proteins
- 10:30 TSONG: Electric energy enforced conformational oscillations of membrane proteins for energy and signal transductions
- 11:30 Lunch

Channels

- 1:00 PM COLOMBINI: Insights into how electric fields can control the structure of membrane proteins from studies on the mitochondrial channel, VDAC
- 1:30 HUANG: Alamethecin and gramicidin channels
- 2:00 - (coffee)
- 2:30 MARSHALL: Helical transitions in peptides as possible gating mechanisms
- 3:00 VODYANOY: Alamethecin - a voltage dependent ion channel
- 3:30 WEBB: Conformational dynamics of a transmembrane channel

THURSDAY, OCTOBER 25

Sensing and Detection

- 8:30 AM FESENKO: Photo reception and olfaction
9:00 KALMIJN: Transduction of nanovolt signals: limits of electric-field detection

9:30 (coffee)

10:00 LOEW: Imaging membrane potential on nonexcitable cells
10:30 PARSEGIAN: Seventy water molecules: unrecognized actors in the hemoglobin play

11:30 Lunch

Electroporation and Electrofusion

- 1:00 PM ABIDOR: Cell contact and Electrofusion
1:30 CHERNOMORDIK: Electropores in lipid bilayers and cell membranes
2:00 CHIZMADZHEV: Mechanism of electrotransfection of animal cells

2:30 (coffee)

3:00 DIMITROV: Mechanisms of membrane electrofusion and electroporation
3:30 SOWERS: What is membrane electrofusion and why do I study it?
4:00 ZELENIN: Electrofusion: new approaches, mechanisms, applications and comparison of DNA electrotransfection with Biostatic technology

FRIDAY, OCTOBER 26

Charges, Fields, & Membranes

- 8:30 AM BUDKER: Interaction of neutrally charged liposomes with polynucleotides in the presence of divalent cations
- 9:00 MCLAUGHLIN: Electrostatics, dimensionality, stoichiometry, cooperativity and the binding of basic amino acids in peptides and proteins to acidic phospholipids in membranes
- 9:30 (coffee)
- 10:00 FOSTER: Dielectrophoresis and levitation of cells: how are they related and what do they show?
- 10:30 PASTUSHENKO: Theoretical investigation of DNA translocation through the cell membrane
- 11:30 Lunch
- 1:00 PM SJODIN: Ion transport across excitable cell membranes studied with tracers
- 1:30 TEISSIE: Lateral proton conduction along lipid monolayers at the air/water interface

CELL CONTACTS AND ELECTROFUSION

I.G.ABIDOR

A.N.Frumkin Institute of Electrochemistry of the USSR Academy of Sciences
Moscow

It is common accepted that efficiency of cell electrofusion is higher when cells are preliminary brought in closer contact. On this base two new approaches in cell electrofusion have been developed. The first one, fusion of cells on an electroconductive (cellulose) film, is very effective for spreading cells (e.g. mouse L-cells) that are able to attach to solid surfaces. The second, more universal, approach is electrofusion of cells in centrifugated pellets. Specific features of cell contacts and possible mechanism of electrofusion are discussed. Electric fields are supposed to initiate fusion process only in areas where plasma membranes of contacting cells are divided narrow extended gaps. These double-membrane structures have high electric and hydrodynamic lateral resistances. Being applied to such a structure electric field promotes bringing of membranes in closer contact, bearing concentric pores in the contacting membranes, bending and pressing edges of pores toward each other. As a result the pore edges are fused to form the membrane tube connecting both membranes and cytoplasm. The cell contacts in the form of the double-membrane structures may also considerable effect on the osmotic behaviour of cell systems. If, by any reason, there are osmotic flows of water in cells the pressure between the contacting membranes drops pressing them to each other. This dynamic osmotic effect can lead to narrowing of the intracellular contacts in cell pellets and increasing of electrical resistance of cell pellets after moderate pulse electrotreatment.

(2) K.J. - 1000, 2000, 4000, 6000, 8000, 10000, 12000, 14000, 16000, 18000, 20000, 22000, 24000, 26000, 28000, 30000, 32000, 34000, 36000, 38000, 40000, 42000, 44000, 46000, 48000, 50000, 52000, 54000, 56000, 58000, 60000, 62000, 64000, 66000, 68000, 70000, 72000, 74000, 76000, 78000, 80000, 82000, 84000, 86000, 88000, 90000, 92000, 94000, 96000, 98000, 100000, 102000, 104000, 106000, 108000, 110000, 112000, 114000, 116000, 118000, 120000, 122000, 124000, 126000, 128000, 130000, 132000, 134000, 136000, 138000, 140000, 142000, 144000, 146000, 148000, 150000, 152000, 154000, 156000, 158000, 160000, 162000, 164000, 166000, 168000, 170000, 172000, 174000, 176000, 178000, 180000, 182000, 184000, 186000, 188000, 190000, 192000, 194000, 196000, 198000, 200000, 202000, 204000, 206000, 208000, 210000, 212000, 214000, 216000, 218000, 220000, 222000, 224000, 226000, 228000, 230000, 232000, 234000, 236000, 238000, 240000, 242000, 244000, 246000, 248000, 250000, 252000, 254000, 256000, 258000, 260000, 262000, 264000, 266000, 268000, 270000, 272000, 274000, 276000, 278000, 280000, 282000, 284000, 286000, 288000, 290000, 292000, 294000, 296000, 298000, 300000, 302000, 304000, 306000, 308000, 310000, 312000, 314000, 316000, 318000, 320000, 322000, 324000, 326000, 328000, 330000, 332000, 334000, 336000, 338000, 340000, 342000, 344000, 346000, 348000, 350000, 352000, 354000, 356000, 358000, 360000, 362000, 364000, 366000, 368000, 370000, 372000, 374000, 376000, 378000, 380000, 382000, 384000, 386000, 388000, 390000, 392000, 394000, 396000, 398000, 400000, 402000, 404000, 406000, 408000, 410000, 412000, 414000, 416000, 418000, 420000, 422000, 424000, 426000, 428000, 430000, 432000, 434000, 436000, 438000, 440000, 442000, 444000, 446000, 448000, 450000, 452000, 454000, 456000, 458000, 460000, 462000, 464000, 466000, 468000, 470000, 472000, 474000, 476000, 478000, 480000, 482000, 484000, 486000, 488000, 490000, 492000, 494000, 496000, 498000, 500000, 502000, 504000, 506000, 508000, 510000, 512000, 514000, 516000, 518000, 520000, 522000, 524000, 526000, 528000, 530000, 532000, 534000, 536000, 538000, 540000, 542000, 544000, 546000, 548000, 550000, 552000, 554000, 556000, 558000, 560000, 562000, 564000, 566000, 568000, 570000, 572000, 574000, 576000, 578000, 580000, 582000, 584000, 586000, 588000, 590000, 592000, 594000, 596000, 598000, 600000, 602000, 604000, 606000, 608000, 610000, 612000, 614000, 616000, 618000, 620000, 622000, 624000, 626000, 628000, 630000, 632000, 634000, 636000, 638000, 640000, 642000, 644000, 646000, 648000, 650000, 652000, 654000, 656000, 658000, 660000, 662000, 664000, 666000, 668000, 670000, 672000, 674000, 676000, 678000, 680000, 682000, 684000, 686000, 688000, 690000, 692000, 694000, 696000, 698000, 700000, 702000, 704000, 706000, 708000, 710000, 712000, 714000, 716000, 718000, 720000, 722000, 724000, 726000, 728000, 730000, 732000, 734000, 736000, 738000, 740000, 742000, 744000, 746000, 748000, 750000, 752000, 754000, 756000, 758000, 760000, 762000, 764000, 766000, 768000, 770000, 772000, 774000, 776000, 778000, 780000, 782000, 784000, 786000, 788000, 790000, 792000, 794000, 796000, 798000, 800000, 802000, 804000, 806000, 808000, 810000, 812000, 814000, 816000, 818000, 820000, 822000, 824000, 826000, 828000, 830000, 832000, 834000, 836000, 838000, 840000, 842000, 844000, 846000, 848000, 850000, 852000, 854000, 856000, 858000, 860000, 862000, 864000, 866000, 868000, 870000, 872000, 874000, 876000, 878000, 880000, 882000, 884000, 886000, 888000, 890000, 892000, 894000, 896000, 898000, 900000, 902000, 904000, 906000, 908000, 910000, 912000, 914000, 916000, 918000, 920000, 922000, 924000, 926000, 928000, 930000, 932000, 934000, 936000, 938000, 940000, 942000, 944000, 946000, 948000, 950000, 952000, 954000, 956000, 958000, 960000, 962000, 964000, 966000, 968000, 970000, 972000, 974000, 976000, 978000, 980000, 982000, 984000, 986000, 988000, 990000, 992000, 994000, 996000, 998000, 1000000, 1002000, 1004000, 1006000, 1008000, 1010000, 1012000, 1014000, 1016000, 1018000, 1020000, 1022000, 1024000, 1026000, 1028000, 1030000, 1032000, 1034000, 1036000, 1038000, 1040000, 1042000, 1044000, 1046000, 1048000, 1050000, 1052000, 1054000, 1056000, 1058000, 1060000, 1062000, 1064000, 1066000, 1068000, 1070000, 1072000, 1074000, 1076000, 1078000, 1080000, 1082000, 1084000, 1086000, 1088000, 1090000, 1092000, 1094000, 1096000, 1098000, 1100000, 1102000, 1104000, 1106000, 1108000, 1110000, 1112000, 1114000, 1116000, 1118000, 1120000, 1122000, 1124000, 1126000, 1128000, 1130000, 1132000, 1134000, 1136000, 1138000, 1140000, 1142000, 1144000, 1146000, 1148000, 1150000, 1152000, 1154000, 1156000, 1158000, 1160000, 1162000, 1164000, 1166000, 1168000, 1170000, 1172000, 1174000, 1176000, 1178000, 1180000, 1182000, 1184000, 1186000, 1188000, 1190000, 1192000, 1194000, 1196000, 1198000, 1200000, 1202000, 1204000, 1206000, 1208000, 1210000, 1212000, 1214000, 1216000, 1218000, 1220000, 1222000, 1224000, 1226000, 1228000, 1230000, 1232000, 1234000, 1236000, 1238000, 1240000, 1242000, 1244000, 1246000, 1248000, 1250000, 1252000, 1254000, 1256000, 1258000, 1260000, 1262000, 1264000, 1266000, 1268000, 1270000, 1272000, 1274000, 1276000, 1278000, 1280000, 1282000, 1284000, 1286000, 1288000, 1290000, 1292000, 1294000, 1296000, 1298000, 1300000, 1302000, 1304000, 1306000, 1308000, 1310000, 1312000, 1314000, 1316000, 1318000, 1320000, 1322000, 1324000, 1326000, 1328000, 1330000, 1332000, 1334000, 1336000, 1338000, 1340000, 1342000, 1344000, 1346000, 1348000, 1350000, 1352000, 1354000, 1356000, 1358000, 1360000, 1362000, 1364000, 1366000, 1368000, 1370000, 1372000, 1374000, 1376000, 1378000, 1380000, 1382000, 1384000, 1386000, 1388000, 1390000, 1392000, 1394000, 1396000, 1398000, 1400000, 1402000, 1404000, 1406000, 1408000, 1410000, 1412000, 1414000, 1416000, 1418000, 1420000, 1422000, 1424000, 1426000, 1428000, 1430000, 1432000, 1434000, 1436000, 1438000, 1440000, 1442000, 1444000, 1446000, 1448000, 1450000, 1452000, 1454000, 1456000, 1458000, 1460000, 1462000, 1464000, 1466000, 1468000, 1470000, 1472000, 1474000, 1476000, 1478000, 1480000, 1482000, 1484000, 1486000, 1488000, 1490000, 1492000, 1494000, 1496000, 1498000, 1500000, 1502000, 1504000, 1506000, 1508000, 1510000, 1512000, 1514000, 1516000, 1518000, 1520000, 1522000, 1524000, 1526000, 1528000, 1530000, 1532000, 1534000, 1536000, 1538000, 1540000, 1542000, 1544000, 1546000, 1548000, 1550000, 1552000, 1554000, 1556000, 1558000, 1560000, 1562000, 1564000, 1566000, 1568000, 1570000, 1572000, 1574000, 1576000, 1578000, 1580000, 1582000, 1584000, 1586000, 1588000, 1590000, 1592000, 1594000, 1596000, 1598000, 1600000, 1602000, 1604000, 1606000, 1608000, 1610000, 1612000, 1614000, 1616000, 1618000, 1620000, 1622000, 1624000, 1626000, 1628000, 1630000, 1632000, 1634000, 1636000, 1638000, 1640000, 1642000, 1644000, 1646000, 1648000, 1650000, 1652000, 1654000, 1656000, 1658000, 1660000, 1662000, 1664000, 1666000, 1668000, 1670000, 1672000, 1674000, 1676000, 1678000, 1680000, 1682000, 1684000, 1686000, 1688000, 1690000, 1692000, 1694000, 1696000, 1698000, 1700000, 1702000, 1704000, 1706000, 1708000, 1710000, 1712000, 1714000, 1716000, 1718000, 1720000, 1722000, 1724000, 1726000, 1728000, 1730000, 1732000, 1734000, 1736000, 1738000, 1740000, 1742000, 1744000, 1746000, 1748000, 1750000, 1752000, 1754000, 1756000, 1758000, 1760000, 1762000, 1764000, 1766000, 1768000, 1770000, 1772000, 1774000, 1776000, 1778000, 1780000, 1782000, 1784000, 1786000, 1788000, 1790000, 1792000, 1794000, 1796000, 1798000, 1800000, 1802000, 1804000, 1806000, 1808000, 1810000, 1812000, 1814000, 1816000, 1818000, 1820000, 1822000, 1824000, 1826000, 1828000, 1830000, 1832000, 1834000, 1836000, 1838000, 1840000, 1842000, 1844000, 1846000, 1848000, 1850000, 1852000, 1854000, 1856000, 1858000, 1860000, 1862000, 1864000, 1866000, 1868000, 1870000, 1872000, 1874000, 1876000, 1878000, 1880000, 1882000, 1884000, 1886000, 1888000, 1890000, 1892000, 1894000, 1896000, 1898000, 1900000, 1902000, 1904000, 1906000, 1908000, 1910000, 1912000, 1914000, 1916000, 1918000, 1920000, 1922000, 1924000, 1926000, 1928000, 1930000, 1932000, 1934000, 1936000, 1938000, 1940000, 1942000, 1944000, 1946000, 1948000, 1950000, 1952000, 1954000, 1956000, 1958000, 1960000, 1962000, 1964000, 1966000, 1968000, 1970000, 1972000, 1974000, 1976000, 1978000, 1980000, 1982000, 1984000, 1986000, 1988000, 1990000, 1992000, 1994000, 1996000, 1998000, 2000000, 2002000, 2004000, 2006000, 2008000, 2010000, 2012000, 2014000, 2016000, 2018000, 2020000, 2022000, 2024000, 2026000, 2028000, 2030000, 2032000, 2034000, 2036000, 2038000, 2040000, 2042000, 2044000, 2046000, 2048000, 2050000, 2052000, 2054000, 2056000, 2058000, 2060000, 2062000, 2064000, 2066000, 2068000, 2070000, 2072000, 2074000, 2076000, 2078000, 2080000, 2082000, 2084000, 2086000, 2088000, 2090000, 2092000, 2094000, 2096000, 2098000, 2100000, 2102000, 2104000, 2106000, 2108000, 2110000, 2112000, 2114000, 2116000, 2118000, 2120000, 2122000, 2124000, 2126000, 2128000, 2130000, 2132000, 2134000, 2136000, 2138000, 2140000, 2142000, 2144000, 2146000, 2148000, 2150000, 2152000, 2154000, 2156000, 2158000, 2160000, 2162000, 2164000, 2166000, 2168000, 2170000, 2172000, 2174000, 2176000, 2178000, 2180000, 2182000, 2184000, 2186000, 2188000, 2190000, 2192000, 2194000, 2196000, 2198000, 2200000, 2202000, 2204000, 2206000, 2208000, 2210000, 2212000, 2214000, 2216000, 2218000, 2220000, 2222000, 2224000, 2226000, 2228000, 2230000, 2232000, 2234000, 2236000, 2238000, 2240000, 2242000, 2244000, 2246000, 2248000, 2250000, 2252000, 2254000, 2256000, 2258000, 2260000, 2262000, 2264000, 2266000, 2268000, 2270000, 2272000, 2274000, 2276000, 2278000, 2280000, 2282000, 2284000, 2286000, 2288000, 2290000, 2292000, 2294000, 2296000, 2298000, 2300000, 2302000, 2304000, 2306000, 2308000, 2310000, 2312000, 2314000, 2316000, 2318000, 2320000, 2322000, 2324000, 2326000, 2328000, 2330000, 2332000, 2334000, 2336000, 2338000, 2340000, 2342000, 2344000, 2346000, 2348000, 2350000, 2352000, 2354000, 2356000, 2358000, 2360000, 2362000, 2364000, 2366000, 2368000, 2370000, 2372000, 2374000, 2376000, 2378000, 2380000, 2382000, 2384000, 2386000, 2388000, 2390000, 2392000, 2394000, 2396000, 2398000, 2400000, 2402000, 2404000, 2406000, 2408000, 2410000, 2412000, 2414000, 2416000, 2418000, 2420000, 2422000, 2424000, 2426000, 2428000, 2430000, 2432000, 2434000, 2436000, 2438000, 2440000, 2442000, 2444000, 2446000, 2448000, 2450000, 2452000, 2454000, 2456000, 2458000, 2460000, 2462000, 2464000, 2466000, 2468000, 2470000, 2472000, 2474000, 2476000, 2478000, 2480000, 2482000, 2484000, 2486000, 2488000, 2490000, 2492000, 2494000, 2496000, 2498000, 2500000, 2502000, 2504000, 2506000, 2508000, 2510000, 2512000, 2514000, 2516000, 2518000, 2520000, 2522000,

Physics of ATP Formation in the Energy-transducing Membranes of
Mitochondria and Chloroplasts

(Theses of presume report)

1. Isolated ATPases from different sources (CF_1 factor from chloroplasts of higher plants, ATPase from *Lactobacillus kassey*, myosin ATPase, etc.) are able to synthesize ATP from ADP and P_i after jump-like increase of the solution pH value.

2. The obligatory condition of ATP synthesis is in this case deprotonization of certain acid groups in the enzyme molecule. This leads to the appearance of the enzyme conformationally non-equilibrium state during relaxation of which the energy-accepting act of tightly bound ATP liberation takes place.

3. New scheme of stationary ATP formation in the processes oxidative phosphorylation in mitochondria and photosynthetic phosphorylation in chloroplasts is proposed.

4. Analysis of chemical reactions within small vesicles by methods of statistical thermodynamics has shown that in such vesicles mass action law breaks down. This compels us to reconsider the thermodynamics of transmembrane particles transfer in these cases.

Main topics of interests: physical mechanisms of enzyme catalysis and intracellular energy transduction.

Background: physical chemistry, quantum chemistry, general biophysics, ESR spectroscopy.

References

1. L.A.Blumenfeld "Problems of Biological Physics", Springer, 1981
2. L.A.Blumenfeld "Physics of Bioenergetic Processes", Springer, 1982
3. L.A.Blumenfeld, D.S.Burbayev, R.M.Davydov "Processes of Conformational Relaxation in Enzyme Catalysis", in: "The Fluctuating Enzyme", Ed. G.R.Welch, John Wiley & Sons, N.Y. 1986.

INTERACTION OF NEUTRALLY CHARGED LIPOSOMES WITH POLYNUCLEOTIDES IN THE PRESENCE OF DIVALENT CATIONS

V.G.Budker

Novosibirsk Institute of Bioorganic Chemistry, Siberian Division of the USSR Academy of Sciences, Novosibirsk, USSR

Large unilamellar liposomes (LUL) composed either of lecithin or lecithin/cholesterol mixture (7:3, M/M) avidly bind a variety of polynucleotides in the presence of divalent cations. The adsorption results in changes of physico-chemical properties of the polynucleotides. After the dissociation of the polynucleotide-LUL complexes by an excess of EDTA, a part of polynucleotide (2-30%) remains irreversibly bound with LUL. This fraction is resistant to DNase 1 treatment, inaccessible to fluorescent dye ethidium bromide and recovered by osmotic or ultrasonic destruction of LUL, which suggests its location within the LUL. The polynucleotide uptake is not accompanied by fusion of LUL or loss of LUL content and is associated with internalization of LUL membrane. The efficiency of the uptake is dependent on the size and concentration of polynucleotides and LUL, phase state of LUL membrane, concentration of di- or trivalent cations in the medium, osmolarity inside the LUL as compared to that outside the LUL and LUL surface/LUL volume ratio. It can be significantly enhanced by applying a short-term electric field to the incubation mixture. A model of the uptake has been proposed which involves the following steps: (i) adsorption of polynucleotide molecules or clusters of the molecules onto LUL surface; (ii) formation of polynucleotide-containing invaginations in LUL membrane; (iii) closing up the invaginations and separation of resulting vesicles inward the LUL. The model gains support from electron microscopic analysis of DNA-LUL complexes formed in the presence of UO_2^{2+} -ions, by which DNA-containing membrane invaginations and vesicles within the LUL have been revealed. In addition to polynucleotides, small negatively charged liposomes have been shown to be uptaken into LUL as well, evidently, by the same mechanism.

ELECTROPORES IN LIPID BILAYERS AND CELL MEMBRANES. L.V. Chernomordik, Frumkin Institute of Electrochemistry, Academy of Sciences o the USSR, Moscow, 117071, USSR.

The properties of the electropores as well as the pore formation and evolution regularities for the lipid bilayers (planar membranes and liposomes) and for the membranes of cells (mainly erythrocytes) were investigated. The experimental approaches used in our studies were based on electrical measurements on the single membranes and on the measurements of permeability for suspensions of cells and liposomes. The mechanism of pore arising, characteristic times and sizes in pore evolution will be discussed. We shall consider also the role of cytoskeleton, colloid-osmotic swelling, and electroosmosis that can modify properties of pores in cell membranes. Role of electropores in fusion and transfection of cells by electrical treatment looks not too direct and obvious. The possible mechanisms of the phenomena mentioned will be discussed as well.

MECHANISM OF ELECTROTRANSFECTION OF ANIMAL CELLS

Yu. Chizmadzhev, The A.N. Frumkin Institute of
Electrochemistry, Academy of Science of the USSR, 117071,
Moscow, V-71, Leninsky Prospekt 31

We studied the cell line cos 1 and plasmide PCM 110 which can replicate in these cells. The plasmide contains the gene lac Z responsible for the expression of β -Gal. We measured the activity of β -Gal which is proportional to the efficiency of electrotransfection (transient expression). Concentration of the cells in PBS (Mg^{2+} , Ca^{2+} free) was $10^7/ml$, concentration of the plasmide - $17\mu g/ml$. We used electric pulses 4 kV/cm, $100\mu s$ duration. To elucidate transport stages we investigated the influence of Ficoll 400 on efficiency of electrotransfection (ET). It was shown that ET decreases with increase of the viscosity of the solution. It means that diffusional stage is important.

It is known that inulin inhibit osmotic lysis of the cells. In our experiments we see no inhibition of ET by inulin. So, osmotic influx is not important for ET. Then we had shown that ET depends on time interval t between electric pulse and introduction of the plasmide in cell suspension: ET increases with the time of preincubation, at $t > 0$, ET is small but $\neq 0$. ET increases with T and decreases under influence of Mg^{2+} . Using DNAase we had shown that DNA penetrates faster than 0,5 min. Changing polarity of the pulses we had shown that electrophoretic stage is important factor. In conclusion some theoretical estimations of possible mechanisms are considered.

I like to indicate the members of our ET-team:
L. Chernomordik, D. Klenchin, S. Leikin. S. Sukharev.

Biophysics of Transmembrane Electric Fields**Participant: Marco Colombini**

Labs. of Cell Biology
Department of Zoology
University of Maryland
College Park, MD 20742

Insights Into How Electric Fields Can Control the Structure of Membrane Proteins from Studies on the Mitochondrial Channel, VDAC

Electric fields are known to be able to alter the structure and function of proteins. Some proteins, however, seem to be finely tuned to respond to changes in the electric field. These proteins are located within cell membranes where the ultra-thin nature of the structure converts small electrical potential differences into very large electric fields. In addition to their location, these proteins are thought to possess specialized domains that constitute a voltage sensor. This structure would have special properties (charge, strong dipole, ability to move or orient relative to the field, etc.) allowing the protein to respond to relatively small changes in the electric field. Although these ideas are fine in principle, what happens in practice when one examines voltage-dependent proteins?

The VDAC channel [1], located in the outer membrane of mitochondria, is an ideal protein for gaining insight into the molecular basis for voltage dependence. This channel is highly conductive and steeply voltage-dependent but yet is composed of only a small amount of protein (a dimer of 30 kDa subunits). The combination of a large pore size (1.5 nm in radius), small amount of protein, and the requirement to form a wall separating environments of radically different electrical polarizability greatly reduces the possible conformations that the protein can be proposed to take. The availability of primary sequences and the use of site-directed mutations have provided further constraints [1,2]. We now have strong evidence for the molecular nature of the channel in its open state [3] and mounting evidence for the nature of the voltage-dependent gating process.

The open state of the channel is thought to be a cylinder composed of two identical subunits arranged in opposite directions (see figure). The result is a structure with two-fold rotational symmetry around an axis in the plane of the membrane that bisects the protein between the subunits. Each subunit is composed of one transmembrane α helix and 12 transmembrane antiparallel β strands. The major lines of evidence in favor of such a structure [1-3] are: 1) the estimates of pore radius and length, 2) the presence of two voltage-gating processes, one at positive and the other at negative electric fields, 3) the appropriate location of the charged and strongly non-polar amino acids in the folding pattern, 4) the location of prolines and other secondary structure breakers at turns in the pattern, and most importantly 5) the use of site-directed mutations to localize charged residues to the transmembrane spanning domains by looking for changes in the ion selectivity of the channel.

The closed state of the channel is proposed to result from the translocation of a portion of the wall of the channel from a

transmembrane location to a location on the surface of the membrane [1] (see figure). This translocation would result in the movement of charges through the electric field resulting in the voltage-dependent energy change responsible for the observed voltage gating. For simplicity and consistent with current results, we propose that one subunit responds to positive potentials and the other to negative potentials. This mechanism of channel closure is consistent with estimated changes in pore radius and volume and the large change in channel ion selectivity. It also accounts for voltage dependence and how the translocation of a voltage sensor would be coupled to a reduction in channel conductance. Most importantly, this mechanism is supported by site-directed mutations both those that influence and those that do not influence the steepness of the voltage dependence. In addition, mutations in the portion of the channel that is proposed to translocate across the membrane have (as required by the proposed mechanism) twice as great an effect on the selectivity of the open state as they do on that of the closed state.

In the membrane channel, VDAC, a discrete voltage sensor seems to be present but it is not as highly charged as the structure proposed for the voltage-gated Na^+ , K^+ , or Ca^{++} channels. In any event, a discrete protein domain seems to be involved. In the case of VDAC, the linkage between the movement of the sensor and the reduction in channel conductance is straight forward.

The nature of the selectivity filter in a large aqueous pore can be understood by examining the VDAC channel. The use of site-directed mutations has allowed us to selectively introduce, remove, or change the sign of charges on the protein wall forming the aqueous pore. We have found that the changes thus introduced resulted in qualitative alterations of ion selectivity as expected from the change in charge. Quantitatively, the magnitude of the selectivity alteration did, in general parallel the magnitude of the charge change with few exceptions. Multiple changes in charge resulted in a remarkably additive change in ion selectivity [3].

A third aspect of the work addresses the question of how predictions of a membrane protein's secondary and tertiary structure based on its primary structure correspond to reality? This is a particularly important question for membrane proteins where less information is available and yet the non-polar nature of the membrane makes predictions of the folding pattern much more enticing. Some of the rules developed for soluble proteins may not apply, at least not in the same way. The simplicity of the structure of the VDAC channel has allowed us to test the predictions made based on the primary sequence. With a conservative predictive approach we obtained agreement between experiments and most predictions but, not surprisingly, a few clear disagreements were also encountered.

References:

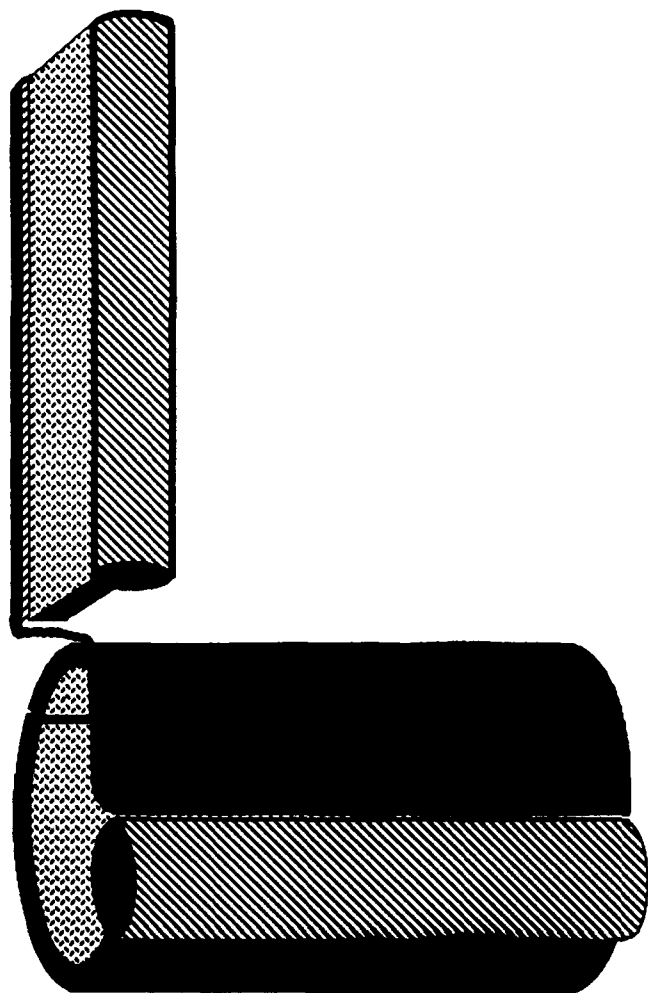
1. Colombini, M. 1989. Voltage gating in the mitochondrial channel, VDAC. Journal of Membrane Biology, 111: 103-111.

COLOMBINI

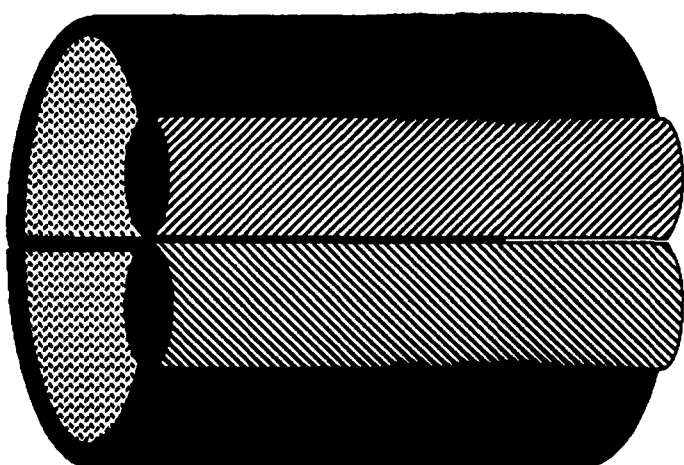
2. Blachly-Dyson, E., Peng, S. Z., Colombini, M. and Forte, M. 1989. Probing the structure of the mitochondrial channel, VDAC, by site-directed mutagenesis: a progress report. Journal of Bioenergetics and Biomembranes, 21:471-483.

3. Blachly-Dyson, E., Peng, S. Z., Colombini, M. and Forte, M. 1990. Alteration of the selectivity of the VDAC ion channel by site-directed mutagenesis: implications for the structure of a membrane ion channel. Science, 247:1233-1236.

COLOMBINI



C L O S E D



O P E N

ELECTRIC FIELD EFFECTS ON MEMBRANE CONFORMATION

Peter Osman*, Frances Separovic#, Ross Smith⁺ and Bruce Cornell#

CSIRO Div. Food Processing, P.O. Box 52 North Ryde, Sydney, N.S.W. 2113 Australia

* CSIRO Div. Applied Physics, P.O. Box 218 West Lindfield, Sydney, N.S.W. 2070 Australia

+ Department of Biochemistry, University of Queensland, St Lucia, Qld 4067 Australia

Title Sentence:

The study, by solid state NMR of the effect of electric field on the conformation, morphology and order of membrane lipids and polypeptides.

Research Interests:

Melittin and gramicidin A facilitate the transport of monovalent cations across lipid bilayer membranes. The mechanisms whereby conduction is achieved is very different for the two peptides. Gramicidin A forms end-to-end membrane-spanning β -helical dimers, stabilised by intramolecular CO..HN hydrogen bonds between peptide planes six residues apart. This structure results from the backbone sequence of alternating L and D residues [1]. Melittin is thought to induce ionic conduction through voltage-stimulated insertion into the membrane creating aggregates that form channels [2]. Many differences exist in the properties of these two ionophores including: the voltage dependence of their conductance, the statistics of ion gating, and the effect these compounds have on membrane stability. Of particular interest to this workshop is the conformational and orientational changes which underly these differences and which occur upon the application of a potential gradient across the membrane. The β helix adopted by gramicidin A possesses a very small overall electrical dipole moment owing to the inherent cancellation of the dipole contributions from the individual peptides. By contrast the 3^{10} helix of melittin has a cumulative dipole moment of order 100D.

The present work builds upon a series of studies by solid-state NMR of the organisation and order of gramicidin A and of melittin when they are dispersed in lipid bilayer membranes, aligned on insulating or metal coated glass slides [3,4,5]. Other compounds studied include, phospholipids [6], glycolipids, ubiquinones [7] and the interaction of these species within multilamellar lipid membranes [8,9]. To obtain a quantitative interpretation of the geometry of a specific site it is usually necessary to synthetically incorporate NMR-visible, carbon-13 or deuterium-2 labels. The membrane ionophores, gramicidin A and melittin, have been labelled with carbon-13 nuclei at the

individual peptide carbonyls, providing information on the conformation and order of these ionophores within the membrane environment. Gramicidin A, was additionally labelled at the C2 carbons of the indole ring of the tryptophan side chains [10]. This permitted an estimation of the conformation and order of the ionophore side chains. Also studied has been the effect on the backbone and sidechain order of changing the membrane thickness [11], the lipid class, and the ion concentration within the aqueous component of the phospholipid-gramicidin A dispersions [12].

Our present work is directed towards the study, by NMR, of carbon-13 labelled sites within melittin incorporated at the peptide carbonyl of both leu-16 and leu-4, and changes in the orientation and conformation of melittin upon the application of a trans-membrane electric field. A technique for applying pulsed, charge-balanced potential gradients to multilamellar liposomes has been developed, based on metal coated stacks of glass coverslips. Through the appropriate metal patterning of these slides, when stacked form a series of interdigitated capacitor plates between which the aligned multilamellar dispersions act as a dielectric. Impedance spectroscopy is employed to follow the equilibration of the dispersion and the formation of its optimal impedance. The conductivity of the ion channels is also characterised by standard BLM and patch clamp techniques.

The effects of electric fields on lipid bilayer dispersions reported by Stulen [13], have been repeated and identified as arising from cooperative, morphological changes in the lipid assembly rather than from significant intramolecular conformational changes. Theoretical estimates of the energy of interaction between the electric fields and the dipole moments which exist within the lipid molecules indicate that intramolecular conformational effects would not be apparent until the potential differences are well in excess of the membrane breakdown voltage.

Two approaches will be discussed at the workshop: (a) measurements of the effect of electric fields on the peptides gramicidin A and melittin via observations of the lipid and (b) via direct observation of labelled ionophores.

References:

1. Cornell B.A. 1987. Gramicidin A-phospholipid model systems: a minireview. *J. Bioenergetics and Biomembranes* **19**: 655-676.
2. Kempf C., Klausner R.D., Weinstein J.N., Renswoude J.V., Pincus M. and Blumenthal R. 1982. *The Journal of Biological Chemistry* **257**: 2469-2476.
3. Smith R. and Cornell B.A. 1986. Dynamics of the intrinsic membrane polypeptide gramicidin A in phospholipid bilayers. *Biophysics J.* **49**: 118-121.

4. Smith R., Thomas D.E., Separovic F., Atkins A. R. and Cornell B.A. 1989. Determination of the structure of a membrane-incorporated ion channel. *Biophysics J.* 56: 307-314.
 5. Cornell B.A., Separovic F., Baldassi A.J. and Smith R. 1989. Conformation and orientation of gramicidin A in oriented lipid bilayers measured by solid-state carbon-13 NMR. *Biophys. J.* 53: 67-76.
 6. Braach-Maksvytis V.L.B. and Cornell B.A. 1988. Chemical shift anisotropies obtained from aligned egg yolk phosphatidylcholine by solid-state C-13 nuclear magnetic resonance. *Biophysics J.* 53: 839-843.
 7. Cornell B.A., Keniry M.A., Post A., Robertson R.N., Weir L.E. and Westerman P.W. 1987. Location and activity of ubiquinone 10 and ubiquinone analogues in model and biological membranes. *Biochemistry* 26: 7702-7707.
 8. Cornell B.A. and Keniry M. 1983. The effect of cholesterol and gramicidin A' on the carbonyl groups of dimyristoylphosphatidylcholine dispersions. *Biochimica et Biophysica Acta*: 732. 705-710.
 9. Cornell B.A., Weir L.E., and Separovic F. 1988. The effect of gramicidin A on phospholipid bilayers. *Eur. Biophys J.* 16: 113-119.
 10. Cornell B.A., Separovic F. and Smith R. 1988. Side chain and backbone conformation of gramicidin A in lipid bilayer membranes. "Transport Through Membranes: Carriers Channels and Pumps", A. Pullman, J. Jortner and B. Pullman (eds), Kluwer Academic Publishers, Dordrecht, 289-295.
 11. Cornell B.A., Separovic F., Thomas D.E., Atkins A.R. and Smith R.S. 1989. Effect of acyl chain length on the structure and motion of gramicidin A. *Biochimica et Biophysica Acta*, 985: 229-232.
 12. Smith R.S., Thomas D.E., Atkins A.R., Separovic F. and Cornell B.A. 1990. Solid-state C-13 NMR studies of the effects of sodium ions on the gramicidin A ion channel. *Biochimica et Biophysica Acta*, *in press*.
 13. Stulen G. 1981. Electric field effects on lipid membrane structure. *Biochimica et Biophysica Acta*, 640: 621-627.
-

MECHANISMS OF MEMBRANE ELECTROFUSION AND ELECTROPORATION:

Dimitter S. Dimitrov+ and Arthur E. Sowers

American Red Cross, Holland Laboratory/Cell Biology
15601 Crabbs Branch Way
Rockville, Md 20855

ABSTRACT: Fusion requires membrane contact and destabilization. Electric fields were used to achieve both because: i) they can be precisely and easily controlled, ii) they are very fast, iii) the close membrane apposition can be reversible and iv) the membrane-membrane contact, the fusogen and the chemistry of the medium can be manipulated relatively independently of one another. To understand mechanisms of membrane fusion we investigated i) destabilization of membranes by high voltage pulses - membrane electroporation monitored by the transfer of the water soluble FITC-dextran, ii) approach and contact of DiI-labeled membranes induced by AC fields and iii) kinetics of fusion of DiI-labeled with unlabeled membranes, recorded by low light level video microscopy.

The main results are:

I. Electroporation

1. There is no delay in the transfer of the labeled dye from the cytoplasmic compartment of the erythrocyte ghosts (time resolution 17 ms - one video frame). Formation of large pores (radius larger than 2.3 nm) is fast.

2. Electroosmosis is the dominant mechanism of molecular exchange in electroporation of erythrocyte ghosts. The hydrodynamic flows through the pores are very fast - rates of the order of 1 m/s.

3. Bending of membranes around pores can be induced by inertial forces due to hydrodynamic flows after the pulse. Formation of such microfunnel membrane structures with heights of the order of 10 nm was recently confirmed by electron microscopy of membranes frozen within 3 ms after the pulse (Chang and Reese, Biophys. J. (1989) 55: 136a).

II. Membrane approach by dielectrophoresis

1. There is time delay to get membranes at contact by electric fields due mainly to the viscous resistance of the liquid layer between the membranes.

2. The delay increases with the increase of the medium viscosity and decrease of the electric field strength.

3. The force of intermembrane attraction strongly increases with increasing the field strength and decreasing the membrane separation.

4. The membranes bend at close apposition. The membrane bending increases the time delay.

III. Membrane electrofusion

1. Reproducible delays between the application of a pulse and first detection of fluorescence in the unlabeled adjacent membranes were found.

2. The delay decreases with an increase of the field strength, decrease of the medium viscosity and decrease of the intermembrane separation.

3. The delay in electrofusion resembles the delay in fusion of vesicular stomatitis viruses with red blood cells (Blumenthal et al. (1989) Conclusion The delay may reflect a long-lived intermediate state in electrofusion. It can be partly due to the mutual approach of membranes to reach molecular contact and/or relatively slow molecular rearrangements leading to membrane merging after the pulse and formation of intermembrane channels or more complicated fusion complexes, where the membrane bending can be important.

PHOTOTRANSDUCTION IN VERTEBRATES: REGULATION OF CATIONIC CONDUCTANCE IN PLASMA MEMBRANE OF ROD OUTER SEGMENTS BY cGMP AND TRANSDUCIN PREPARATION. E. Fesenko, Institute of Biological Physics, USSR Academy of Sciences, Pushchino, Moscow Region, 142292, USSR.

The Main Results in Sensory Reception

In Photoreception:

Confirmation of the mediator role of cGMP in vertebrate phototransduction by patch-clamp method. It was shown that cGMP directly (without phosphorylation of protein substrates) regulates the cationic conductance of the plasma membrane.

The cGMP-sensitive channel possesses the smallest (0.1 pS) unitary conductance of any channel yet studied. According to this fact, the plasma membrane of rod outer segments contains a great number of open channels. This may explain the low level of noise of the photoreceptor cell. The matter is that the relative value of noise is equal to $1/N$, where N - the number of open channels. The cGMP-activated conductance may be completely and reversibly suppressed by transducin preparation, obviously, at the expense of direct inhibition of the open channel by transducin. The anti-idiotypic antibodies for the channels have been obtained. These antibodies modulate the cGMP sensitive conductance and could be used to isolate the channel and study the properties.

The new fast conformational rearrangement in rhodopsin was found. This led to demasking the retinal-opsin NC-bond. This "demasking" re-arrangement was isochromic, not associated with known rhodopsin conformational transitions and, judging by its time characteristics (time constant 0.1s at physiological temperatures), it may be of a functional importance; for example, it may play a key role in switching off the light-induced state of rhodopsin, activating transducin. (along with the process initiated by 48 kDa protein).

In Olfaction:

The specific membrane glycoproteins (molecular mass 140 kDa) with high affinity for odorants ($K_D = 10^{-10} - 10^{-6} M$) were isolated from olfactory epithelium of different animals (frog, rat, carp and scate). They consisted of two subunits (88 - 98 kDa and 55 kDa). The 88 - 98 kDa subunit has a binding to odorants. Antibodies to these glycoproteins inhibited both the electroolfactogram and the binding of odorants showing them to be receptor molecules. The 55 kDa subunit possesses GTP-ase activity, which may be regulated by the 99 kDa subunit bound to a ligand.

SELECTED PUBLICATIONS

1. Vladimirov Yu.A., Fesenko E.E., "On the summation of quanta at the photoionization of tyrosine and triptophan in alkaline solutions", Photochem. Photobiol., 8, 3, 209-212, 1968.
2. Fesenko E.E., "On possible mechanism of transition of two-quantum photoionization of phenol derivatives at 77°K into monoquantum one at the temperature increase", Dokl. AN SSSR, 1181-1183, 1969.
3. Fesenko E.E., Volkenstein M.V., Kulakov V.N., Lyubarasky A.L., "The three-phase kinetics of mioglobin recombination with carbogen oxide at low temperatures", Dokl. AN SSSR, v.205, No. 2, 487-488, 1972.

4. Fesenko E.E., Lyubarsky A.L., "Effect of light on artificial lipid membrane modified by the photoreceptor membrane fragments", Nature, 268, 5620, 562-563, 1977.
5. Fesenko E.E., Kolesnikov S.S., Lyubarsky A.L., "Induction by cyclic GMP of cationic conductance in plasma membrane of retina rod outer segment", Nature, V.313, N 6001, 310-313, 1985.
6. Fesenko E.E., Novoselov V.I., Bystrova M.F., "The subunits of specific odor-binding glycoproteins from rat olfactory epithelium", FEBS Letters, V.219, No.1, 224-226, 1987.
7. Krapivinsky G.B., Filatov G.N., Filatova E.A., Lyubarsky A.L. and Fesenko E.E. "Regulation of cGMP-dependent conductance in cytoplasmic membrane of rod outer segments by transduction. FEBS Letters No. 2, V. 247, 435-437.

THE TRANSDUCTION OF PROTEIN-LIGAND BINDING ENERGY INTO DRIVING FORCES FOR
CATALYTIC, MECHANICAL, CONFORMATIONAL, AND OTHER FORMS OF BIOLOGICAL WORK

Harvey F. Fisher and Narinder Singh, U. of Kansas Med. Cent., VA Med. Cent.,
4801 Linwood Blvd., Kansas City, MO 64128, (816) 861-4700 X3455.

The idea that enzyme-ligand binding energy can somehow be converted into a catalytic driving force, originally suggested by Pauling (1), is now widely accepted. Elegant theories based on this idea have been developed, but they are not subject to experimental testing (2). Lumry (3) has suggested a mechanism for such energy transduction in which ligand-induced changes in protein free energy are arranged to be complementary to the corresponding features for the chemical reaction coordinate (Fig. 1). We have found a specific enthalpic signal which permits us to track a ligand-induced, highly energetic protein macrostate transition in pyridine nucleotide dehydrogenases which appear to fulfill Lumry's criterion of complementarity.

The High Enthalpy, Ligand Induced Transitions. The phenomenon are described in detail in reference 4, and are summarized here: 1. All of the many binary and ternary complexes of glutamate dehydrogenase (GDH) are characterized by the presence of a two-state transition whose ΔH is invariably 22,000 cal. mol^{-1} , but whose T° values (which are ΔG° functions vary widely among the various enzyme forms, as shown in Fig. 2A. 2. The distinctive shape of the temperature dependence of the enthalpy from such two state-transitions as seen in Fig. 2A, permits the assignment of the changes in ΔG° of the enzyme molecule itself induced by the various ligands (coenzymes, substrates, modifiers, H^+ , etc.) as shown in Fig. 2B. 3. A set of such protein-component ΔG° 's obtained for the various enzyme complexes that occur along the reaction path provides us for the first time with the opportunity to actually isolate the heretofore hypothetical component shown as the dashed line in Fig. 1.

Energy Transduction Machinery in Enzyme Reactions. It is easily shown that the occurrence of such ligand induced two-state transitions does increase the ΔG° of the protein at the expense of some of the ΔG° of binding of the ligand. This does not, however, constitute storage in any real sense and is not in itself sufficient to constitute an energy transduction machine. The minimal requirements for such a machine are: 1. an energy input step, 2. a transmission step (or steps), 3. a power stroke, 4. a return step.

A Proposed Transduction Model for the Energetics of the GDH Reaction. A machine of the sort we propose has two essential features. If each of the enzyme forms along the reaction pathway has the particular " T_o " necessary at that point in the sequence, then that series of interconversions between their high and low enthalpy forms can constitute the linked four-step machine necessary for the transduction of binding energy into catalytic driving force. A second necessary feature of this machine is the blockage of such interconversions by high energy barriers at certain critical points in the sequence, and the absence of such barriers at other critical points.

The Glutamate Dehydrogenase (GDH) Catalyzed Reaction Viewed as an Energy Transduction Machine. We have found evidence that the complexes of GDH do indeed have these necessary properties. The behavior of the system is shown in Fig. 3. The ΔG° values and degree of displacement of the $E \leftrightarrow E'$ equilibrium for the various complexes were obtained by calorimetric and

free energy measurements as described in reference (4). The operation of this reaction viewed as a machine appears to proceed as follows: A. Energy input step. The binding of R (NADPH) to the enzyme raises the free energy of the protein by about 5 kcal.mol^{-1} at the expense of a correspondingly weakened binding of the coenzyme. B. Transmission step. The binding of K (α -ketoglutarate) to the high energy ER form releases only a part of the energy induced in the system. This partial release accomplishes two functions: it provides a kinetic force to drive the overall reaction at the necessary speed and it tightens the binding of K at the expense of R--a local energy transduction feature. C. Power stroke. The addition of N (NH_3) to ERK initiates the actual chemistry of the reaction, releasing most of the remainder of the original energy input and thereby drives the catalytic step. D. Return step. The energy of the protein in the enzyme product complex is only slightly higher than that of the free enzyme itself, satisfying the necessary condition here. Thus, the system appears to demonstrate binding energy transduction.

The Nature of the $E \leftrightarrow E'$ transition. We have found that the transition itself in this particular system is driven by complex set of proton ionizations (5), involves substantial changes in protein structure, (as shown by large changes in the denaturation properties of the various complexes, and is subject to allosteric control by anion binding site (6). Kodama (7) has observed a very similar temperature-dependent binding enthalpy in the myosin ATPase system and has proposed a model very similar to ours for that well known energy transduction system. Privalov (8) has found such pre-denaturational enthalpic phenomena to be a widespread feature among proteins. There is no reason why the machinery described here (to the extent that it exists at all) should be limited to driving catalysis. It would appear to be applicable to any biological energy transduction process. One such application that can be imagined is the transduction of specific ion binding energy to drive the physical deformation of proteins comprising ion transport channels in membranes.

REFERENCES

1. Pauling, L. Chem. Eng. News 24, 1375 (1946).
2. Jencks, W.P. Advances in Enzymology 43, 219, (1975).
3. Lumry, R.R. in Fluctuating Enzyme, p. 4.
4. Fisher, H.F. in Advances in Enzymology, 61, p. 1, (1988).
5. Fisher, H.F., Maniscalco, S., Wolfe, C., and Srinivasan, R. Biochemistry, 25, 2910, (1986).
6. Chalbi, P., Maniscalco, S., Cohn, L.E., and Fisher, H.F. Biochim. Biophys. Acta, 913, 103, (1987).
7. Kodama, T., Physiol. Rev. 65, 467, (1986),
8. Privalov P. Adv. Prot. Chem. 33, 167, (1979).

This work was supported in part by Grant PCM-8203880 from the National Science Foundation, Grant GM-15188 from the General Medicine Institute of the National Institutes of Health, BRSG S07 RR 05373 awarded by Biomedical Research Support Grant Program, Division of Research Resources, NIH, and by the Veterans Administration.

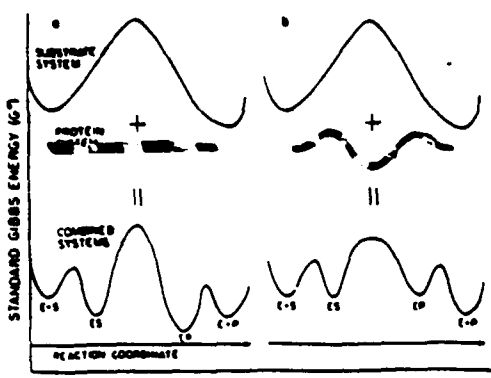


Figure 1

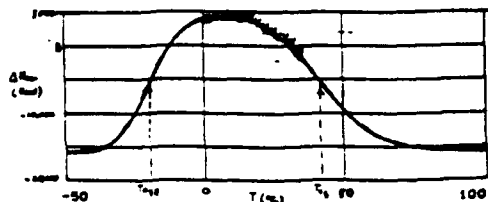
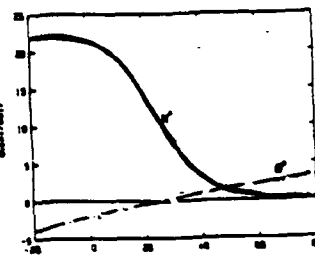


Figure 2A



Page 21

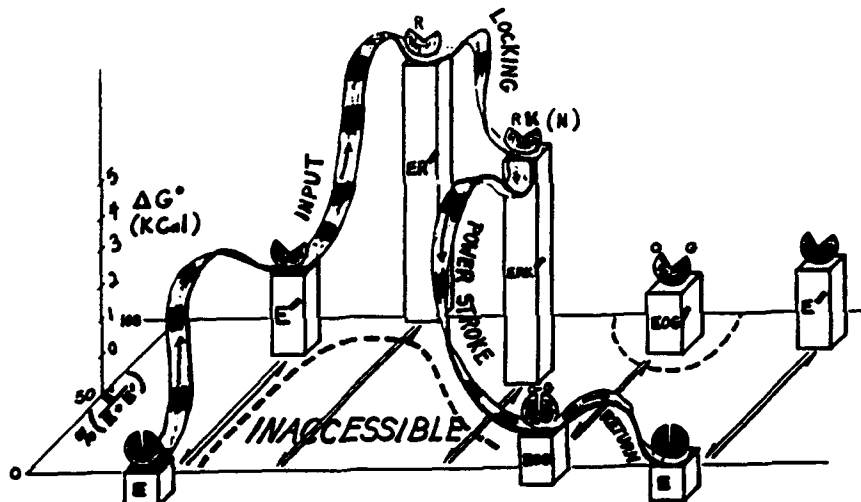


Figure 3

FIGURE LEGENDS

Figure 1. The Luxury "free-energy complementarity" concept. The dashed line represents the level of ligand binding energy stored in the protein molecule itself.

Figure 2. Thermodynamic parameters for a ligand-induced two state protein transition. A. Temperature dependence of H_{observed} for the binding of NADPH to glutamate dehydrogenase. XXX's are experimental points. The line corresponds to eq. (11) of ref. (4). Arrows indicate values of T_0 (the temperature at which $\Delta G^\circ = 0$ for an $E \leftrightarrow E'$ transition) for the enzyme-ligand complex and for the free enzyme respectively. B. The dependence of ΔH° and ΔG° of the protein component alone (observed at 25°C) on the T_0 value for that form.

Figure 3. The liver glutamate dehydrogenase reaction as a ligand-binding-energy transduction machine. The dashed band corresponds to the relative ΔG° of the protein component only, corresponding to the dashed line of Fig. 1. Values of ΔG° and $\Delta E^\circ/(E+E')$ have been calculated from experimental data cited in ref. 4. The values for the reactive EOG and EOG' complexes have been calculated from the properties of the corresponding D-glutamate complexes. E and E' represent the low and high enthalpy states of the various enzyme forms. R is NADPH; K is α -ketoglutarate; N is ammonia; O is NADP; G is glutamate.

FOSTER

D

DIELECTROPHORESIS AND LEVITATION OF CELLS: HOW ARE THEY RELATED AND WHAT DO
THEY SHOW?

Kenneth R. Foster

Department of Bioengineering, University of Pennsylvania
Philadelphia PA 19104-6392

phone:215/898-8534
fax:215/898-1130

D

ABSTRACT

The initial step in the electrofusion process is the field-induced aggregation of cells into pearl chains. This effect arises from the mechanical force exerted on the cell by the applied electric field, but is difficult to analyze rigorously. I review two other kinds of field-induced forces on cells: a linear force acting on a cell located in an inhomogeneous field, and a torque exerted on a cell located in a circularly polarized electric field. Both forces can be described theoretically in terms of a single complex quantity, u^* , which is the induced dipole moment of the cell. A simple theoretical analysis relates these two different forces and shows their relation to the dielectric properties of the cell. The study of field-induced forces can provide important information about electrical properties of cells in suspension.

INTRODUCTION

The initial step in electroporation is the formation of linear aggregates ("pearl chains") of cells using an electric field. The pearl chains are created by the mechanical force exerted on the cells by the field. This phenomena is difficult to analyze, in part because of the complicated field pattern that exists in a concentrated suspension of cells; extensive experimental studies on the effect have been reported by Schwan and colleagues.

I describe two different field-induced forces on cells: linear forces acting on a cell that is located in an inhomogeneous field, and torque exerted on a cell located in a circularly polarized electric field. Both of these effects have been used to study the electrical properties of cells and other small particles [1] [2] [3] [4]. I present a simple analysis that shows the close relationship between these two electromechanical effects and the underlying dielectric properties of the cell.

THEORETICAL BACKGROUND

Consider a particle of dielectric properties (ϵ_p and σ_p) suspended in a medium of properties (ϵ_s and σ_s). The complex permittivity ϵ^* and conductivity σ^* are:

$$\sigma^* = \sigma + j\omega\epsilon \quad (1)$$

$$\epsilon^* = \epsilon - j\sigma/\omega \quad (2)$$

(Complex quantities are denoted by *). The dielectric properties of the suspension (ϵ_s , σ_s) are approximately given by the Maxwell mixture theory: if the dielectric properties of the suspended and continuous phases are (ϵ_p , σ_p) and (ϵ_s , σ_s):

$$\frac{u^*}{(u^*)_s} = \frac{(\epsilon_p^* - \epsilon_s^*)}{(\epsilon_s^* + 2\epsilon_p^*)} = \frac{(\sigma_p^* - \sigma_s^*)}{(\sigma_s^* + 2\sigma_p^*)} \quad (4)$$

$$\frac{(u^*)_s}{(u^*)_p} = \frac{(\epsilon_s^* - \epsilon_p^*)}{(\epsilon_p^* + 2\epsilon_s^*)} = \frac{(\sigma_s^* - \sigma_p^*)}{(\sigma_p^* + 2\sigma_s^*)} = pu^* \quad (3)$$

where p is the volume fraction of the suspension and u^* is the Clausius-Mossotti ratio. Solving Eqs. 3 and 4 to obtain the dielectric properties of the suspension:

$$\sigma_{\infty} = \frac{9p\sigma_p}{(2+p)^2} + \frac{2\sigma_m(1-p)}{(2+p)} - \frac{9p\sigma_p^2(1-p)}{(\sigma_m(2+p) + \sigma_p(1-p))(2+p)^2} \quad (5)$$

In the limit of small p , this reduces to

$$\sigma_{\infty} \approx \sigma_m(1+3pu^*) \quad (6)$$

DIELECTROPHORESIS AND TORQUE

The force F on an uncharged dielectric particle in an inhomogeneous electric field is:

$$F = 2\pi\epsilon_m r^3 \nabla(E^2) Re(u^*) \quad (7)$$

where

$$Re(u^*) = \frac{\omega^2(\epsilon_p - \epsilon_m)(\epsilon_p + 2\epsilon_m) + (\sigma_p - \sigma_m)(\sigma_p + 2\sigma_m)}{\omega^2(\epsilon_p + 2\epsilon_m)^2 + (\sigma_p + 2\sigma_m)^2} \quad (8)$$

This force arises from the interaction between the field and the induced dipole moment of the particle, and is directed towards regions of higher or lower field intensity (positive or negative dielectrophoresis) depending on the sign of the numerator of Eq. (8).

The torque on the particle is given by the cross product of the field vector with the induced dipole moment. In rotation experiments the applied field is circularly polarized, and u^* rotates at the same circular frequency as the field but with a phase lag. In that case the torque is [5]:

$$\tau = 4\pi\epsilon_m r^3 E^2 Im(u^*) \quad (9)$$

where

$$Im(u^*) = \frac{3\omega(\epsilon_p\sigma_m - \epsilon_m\sigma_p)}{\omega^2(2\epsilon_m + \epsilon_p)^2 + (2\sigma_m + \sigma_p)^2} \quad (10)$$

The torque can either be in the same or opposite sense as the rotation of electric field vector (cofield or counterfield torque) depending on the sign of the numerator in Eq. (10).

Both the force and torque are frequency-dependent. A partial fraction expansion of u^* gives

$$u^* = \frac{A}{(s + \omega_m)} + B; \quad (11)$$

with $s = j\omega$. This has a simple pole at the frequency $-\omega_m$ where

$$A = \frac{(\epsilon_m \sigma_p - \epsilon_p \sigma_m)}{(2\epsilon_m + \epsilon_p)^2} \quad (12)$$

$$B = \frac{\epsilon_p - \epsilon_m}{2\epsilon_m + \epsilon_p} \quad (13)$$

$$\omega_m = -(2\sigma_m + \sigma_p)/(2\epsilon_m + \epsilon_p).$$

The real and imaginary parts of u^* are

$$Re(u^*) = A \frac{\omega_m}{\omega^2 + \omega_m^2} + B \quad (14)$$

$$Im(u^*) = \frac{-A\omega}{\omega^2 + \omega_m^2} \quad (15)$$

Thus, the force ($Re(u^*)$) increases (or decreases) monotonically with frequency with a breakpoint at ω_m . The torque ($Im(u^*)$) has a broad peak (which may be positive or negative) at ω_m , and then falls off linearly with frequency. This dispersion (the so-called Maxwell-Wagner dispersion) is observable in the bulk dielectric properties, and arises from the charging of interfaces in the suspension.

Now consider a particle whose dielectric properties are characterized by a single time constant τ' (relaxation frequency $\omega' = 1/\tau'$). Thus,

$$\sigma_p = \sigma_o + (\sigma_m - \sigma_o) \frac{j\omega\tau'}{1 + j\omega\tau'} \quad (16)$$

Expanding u^* by partial fractions yields:

$$u^* = \frac{C}{s + \omega_1} + \frac{D}{s + \omega_2} - \frac{1}{2} \quad (17)$$

In this case the force and torque exhibit two dispersions. The force is described by two monotonic segments with midpoints at ω_1 and ω_2 ; the torque has maxima (or minima) at ω_1 and ω_2 . Expressions for the amplitudes C and D and poles $-\omega_1$ and $-\omega_2$ are algebraically complicated and omitted here.

An interesting case is when $\tau' \gg \tau$. This applies, for example, to dielectric relaxation in cells, which typically show relaxation time constants in the microsecond range [6] [7]. By expanding C, D, ω_1 and ω_2 to first order in ω' we find:

$$C = -\frac{3\omega'\sigma_m(\sigma_m - \sigma_o)}{(\sigma_m + 2\sigma_m)^2} \quad (18)$$

$$D = \frac{3\omega'(\sigma_m - \sigma_o)}{(\sigma_m + 2\sigma_m)^2} + \frac{3\sigma_m}{4\epsilon_m} \quad (19)$$

$$\omega_1 = \frac{\omega'(2\sigma_m + \sigma_o)}{\sigma_m + 2\sigma_m} \quad (20)$$

$$\omega_2 = \frac{\sigma_m + 2\sigma_m}{2\epsilon_m} + \frac{\omega'(\sigma_m - \sigma_o)}{\sigma_m + 2\sigma_m} \quad (21)$$

One term in this expansion corresponds to the Maxwell-Wagner dispersion of the suspension; the other to the dielectric dispersion of the particles.

This analysis can be extended to more complicated systems. Dielectric relaxation of any system can be described as a superposition of first-order processes [8]. Thus, u^* can be expanded into a sum of first order terms. The number of terms (hence the number of relaxations in u^*) exceeds by one the sum of the number of relaxations in each phase.

This analysis allows a simple comparison of the dielectrophoretic and rotation spectra. Each consists of a superposition of first-order processes with peaks (in torque) or midpoints (in force) at frequencies $\omega_1, \omega_2, \dots$ (the poles of u^*). The strength parameters A, B, C, ... are either positive or negative depending on the dielectric properties of the particle vs. the medium.

Membrane covered spheres This result can be readily applied to the case of a membrane-covered sphere, used to model a biological cell. From the Maxwell mixture theory, the effective conductance σ_e of the cell is obtained from [6]

$$\frac{\sigma_e - \sigma_{mem}}{\sigma_e + 2\sigma_{mem}} = \frac{(R - d)^3}{d^3} \frac{\sigma_i - \sigma_{mem}}{\sigma_i + 2\sigma_{mem}} \quad (22)$$

where σ_i and σ_{mem} are the complex conductivities of the interior of the sphere and membrane, and d and R are the thickness of the membrane and radius of the sphere. For a thin membrane ($d \ll R$) this reduces to

$$\sigma_e = \frac{\sigma_i + 2\sigma_{mem} \frac{d}{R}}{1 + \frac{d\sigma_i}{R\sigma_{mem}}} + s\epsilon_i \quad (23)$$

Neglecting the permittivity of the cytoplasm, i.e.

$$\text{Im}(\sigma_i) = 0$$

and defining the membrane capacitance and conductance:

$$C_m = \epsilon_m/d$$

$$G_m = \sigma_m/d$$

leads to the result

$$\frac{1}{\sigma_e} = \frac{1}{\sigma_i} + \frac{1}{R(G_m + sC_m)} \quad (24)$$

This can be written in the form of Eq. 16 with

$$\omega' = 1/\tau' = \frac{1+RG_m/\sigma_i}{C_m R/\sigma_i} \approx \frac{\sigma_i}{C_m R} \quad (25)$$

$$\sigma_{p,o} = \sigma_{c,o} = \frac{RG_m}{1+RG_m/\sigma_i} \approx RG_m \quad (26)$$

$$\sigma_{p,\infty} = \sigma_{c,\infty} = \sigma_i \quad (27)$$

$$\epsilon_{p,\infty} = \epsilon_i \quad (28)$$

Inserting this into Eqs. 18-21 gives

$$\omega_1 = \frac{\omega'(2\sigma_m + G_m R)}{\sigma_i + 2\sigma_m} \approx \frac{\omega'(2\sigma_m)}{\sigma_i + 2\sigma_m} \quad (29)$$

$$\omega_2 = \frac{\sigma_1 + 2\sigma_m}{\epsilon_i + 2\epsilon_m} + \omega' \frac{\sigma_i - RG_m}{\sigma_i + 2\sigma_m}. \quad (30)$$

$$C = \frac{3\omega'\sigma_m(\sigma_i - RG_m)}{(\sigma_i + 2\sigma_m)^2} \quad (31)$$

$$D = 3 \frac{\epsilon_m \sigma_i - \epsilon_p \sigma_m}{(2\epsilon_m + \epsilon_p)^2} + 3 \frac{\sigma_m \omega' (\sigma_i - RG_m)}{(\sigma_i + 2\sigma_m)^2} \quad (32)$$

Of the above equations, Eqs. 30 and 32 depend mostly on the dielectric properties of the medium and cytoplasm; the terms containing ω' (i.e. the membrane properties) are small and probably negligible. In contrast, Eqs. 29 and 31 strongly depend on the membrane properties. Both the levitation and rotation spectra are thus very sensitive indicators of the electrical properties of the cell, particularly the membrane capacitance. They offer complementary approaches for studying the electrical properties of cells.

REFERENCES

- [1] K. V. I. S. Kaler and T. B. Jones, "Dielectrophoretic spectra of single cells determined by feedback-controlled levitation," *Biophys. J.* 57: 173-182 (1990).
- [2] W. M. Arnold and U. Zimmermann, "Electro-rotation: Development of a technique for dielectric measurements on individual cells and particles," *J. Electrostatics* 21: 151-191 (1988).
- [3] R. Glaser and G. Fuhr, "Electrorotation - The spin of cells in rotating high frequency electric fields, in Mechanistic Approaches to Interactions of Electric and Electromagnetic Fields with Living Systems, M. Blank and E. Findl, Eds. Plenum Press, New York NY 1987.
- [4] W. M. Arnold, H. P. Schwan, and U. Zimmermann, "Surface conductance and other properties of latex particles measured by electrorotation," *J. Phys. Chem.* Vol: 91 PP. 5093-5098 (1987).
- [5] F. A. Sauer and R. W. Schlögel, "Torques exerted on cylinders and spheres by external electromagnetic fields," in Interactions between Electromagnetic Fields and Cells (Plenum Press, New York, 1985) pp. 203-251.
- [6] H. P. Schwan, "Electrical properties of tissue and cell suspensions," *Adv. Biol. Med. Phys.* J. H. Lawrence and C. A. Tobias, Eds., Academic Press, NY 141-209 (1957).
- [7] H. P. Schwan, "Determination of Biological Impedances," in Phys. Tech. Biol. Res. 6: 323-407 (1967).
- [8] P. Colonomos and R. G. Gordon, "Bounded error analysis of experimental distributions of relaxation times," *J. Chem. Phys.* 71: 1159-1166 (1979).

(For Int'l Conference on Biophysics of Transmembrane Electric Fields, Oct 23-26, 1990)

ALAMETHICIN AND GRAMICIDIN CHANNELS

Huey W. Huang, Physics Department, Rice University, Houston, TX 77251
[Phone (713) 527 4899; FAX (713) 527 9033; E-mail HUANG@physics.rice.edu]

I would like to discuss in molecular detail two examples of electric field interacting with membrane via ion channels. First on the voltage gating mechanism of the alamethicin channel. Second on x-ray diffraction on the gramicidin channel in membrane.

Alamethicin Channel

Alamethicin, an antibiotic produced by the fungus *Trichoderma viride*, is a linear icosapeptide which spontaneously inserts into black lipid membranes and the membranes of some living cells producing a voltage-dependent ion conductance (Mueller and Rudin, 1968). The peptide forms an amphiphilic helix in crystals, with its polar residues lying along a strip parallel to the axis (Fox and Richards, 1982). In membrane-associated states, perhaps 60-70% of alamethicin residues are in the α -helical form. Presumably the alamethicin channel is a pore formed by an aggregate of such partial helices, similar to the pores in channel proteins. Thus it is of interest to study alamethicin as a simple model of voltage-gated ion channels. Its change of state with voltage may also illuminate the nature of protein-lipid interactions in general.

The assumption that alamethicin monomers form a water-filled conducting pore like the staves of a barrel is supported by most kinetic data of ion conductances (Latorre and Alvarez, 1981). However the conducting state represents only the end state of a voltage-dependent process. In order to understand the voltage-gating mechanism, one also needs to know the initial state, and the intermediate states, if any. Conduction experiments provided no clues for the non-conducting state, either about the location of the molecule (relative to the membrane) or its configuration. Given its molecular structure, four plausible states have been suggested for alamethicin in the absence of an electric field, i.e., dispersed in the aqueous solution, bound parallel to the lipid-water interface, incorporated in the bilayer, or partly incorporated in the bilayer (presumably the α -helical part) and the rest either projecting into the solution or bound to the interface. In each of these states, the peptide may be either monomers or aggregates. Thus there are many alternative theoretical pathways that alamethicin might take in response to an applied electric field, and each may satisfy the voltage dependence of the measured macroscopic conductance. In the last ten years, numerous spectroscopic and other methods have been used to study the non-conducting state, including Raman spectroscopy (Lis et al., 1976; Banerjee et al., 1985; Knoll, 1986), ^1H , ^2H and ^{31}P nuclear magnetic resonance studies (Banerjee et al., 1983; Banerjee et al., 1985), infrared attenuated total reflection spectroscopy (Fringeli and Fringeli, 1979), alamethicin-phospholipid cross-linking studies (Latorre et al., 1981), titration and stopped-flow analyses using circular dichroism (CD) and fluorescence to monitor the alamethicin-lipid interactions (Schwarz et al., 1986; Schwarz et al., 1987; Rizzo et al., 1987); capacitance studies (Vodyanoy et al., 1988), and studies of synthetic analogues (Vodyanoy et al., 1982; Hall et al., 1984; Menestrina et al., 1986). The results have led to many different conclusions. In particular, there are conflicting conclusions as to whether, in the absence of a transmembrane electric field, alamethicin partitions into the apolar region of a lipid bilayer or adsorbs to the lipid-water interface. Lis et al (1976), Banerjee et al. (1983), Banerjee et al. (1985) and Vodyanoy et al (1988) found evidence for interfacial interactions. But Fringeli and Fringeli (1979), Latorre et al. (1981), Knoll (1986), Schwarz et al.(1986), Schwarz et al. (1987) and Rizzo et al. (1987) concluded that alamethicin inserts into bilayers.

Here I report the discovery of a new phenomenon of alamethicin-membrane interactions. We discovered a phase transition between a state in which all alamethicin molecules bind parallel to the membrane surface and a state in which all alamethicin molecules insert perpendicularly into the membrane, as a function of lipid/peptide ratio and of the chemical potential of water. The state of alamethicin was monitored by the newly developed method of oriented circular dichroism (OCD; Wu et al., 1990) using aligned multilayer samples in the liquid crystalline L_α (smectic A) phase (no lipid phase transitions are involved). If the lipid/peptide ratio exceeds a critical value, all alamethicin molecules are on the membrane surface. If the lipid/peptide ratio is below the critical value, all alamethicin molecules are incorporated in the membrane when the degree of hydration is high; when the degree of hydration is low, alamethicin is again on the membrane surface. The fact that all alamethicin molecules are sensitive to the chemical potential of water indicates that alamethicin incorporated in membrane is associated with water, probably all in the water-filled barrel-stave forms. In a typical conduction experiment, alamethicin molecules are partitioned between the aqueous phase and the lipid phase; in the lipid phase, the lipid/peptide ratio is such that alamethicin is on the membrane surface in the absence of a field. As I will show, when an electric field is applied, it is those surface peptides (rather than those in the aqueous phase) which will probabilistically turn into the membrane to form channels. This model is in agreement with most ion conduction data. The confusion and contradiction reported in the literature are due to the lack of information on the dependence of the state of alamethicin on the lipid/peptide ratio and on the type of lipid.

The phase transition can also be understood. Since this is a macroscopic cooperative phenomenon, there must be long-range interactions between peptide molecules in membrane. We believe that an alamethicin channel fits into a bilayer by matching its (exterior) hydrophobic and hydrophilic regions with those of the surrounding lipids; and this fitting causes some distortion of the peptide-free equilibrium configuration of the bilayer. The range of such a distortion can indeed be long (many nanometers; see Huang, 1986); and within that range, the fitting of another channel into the bilayer is facilitated. Such membrane-mediated intermolecular interactions between protein molecules have been discussed before (Marcelja, 1976; Schröder, 1977; Owicki and McConnell, 1979), in particular by Pearson et al. (1984) who used a general (or nonspecific) free energy for membrane deviated from equilibrium, and by Huang (1986) who used the elastic free energy for membrane deformation. I will present a model to qualitatively explain the phase diagram of the phase transition mentioned above (Huang, 1975).

Gramicidin Channel

Gramicidin, a linear pentadecapeptide, is by far the most extensively studied membrane-active peptide which forms a transmembrane ion channel. It is now generally accepted that the gramicidin channel is a cylindrical pore formed by two monomers, each a single-stranded β 6.3 helix and hydrogen-bonded head-to-head at their N-termini (Urry, 1985; Arseniev et al., 1985). The pore selectively facilitates the diffusion of monovalent cations across bilayer membranes, but does not transmit anions and divalent cations (Hladky & Haydon, 1984). There are extensive kinetic data describing the effect on the channel conductivities of a great number of variables including amino acid variation, membrane variation, ion valence variation, cation variation, etc. (Hladky & Haydon, 1984; Andersen, 1984; Andersen et al.; 1987; Koeppe & Andersen, 1987). The relatively simple structure and the wealth of experimental data on its ion conductances make gramicidin an ideal model system for the study of the principles governing ion transport across lipid membranes. In particular, many molecular dynamics computations and simulations have been performed in an attempt to understand the detailed properties of the channel, such as the free energy profiles of ions, the hydrogen bonding pattern of water, the ion and water motions, etc. (Mackay, et al., 1984; Pullman, 1987; Roux and Karplus (1988); Jordan, 1988; Chiu et al.,

1989). Unfortunately, the lack of molecular data for comparison makes it difficult to evaluate these theoretical and computational results. One of the desirable molecular data is the location of the ion binding sites, which, we believe, is the key to the ion selectivity.

I will report the first x-ray diffraction on gramicidin in its membrane-active form by using uniformly aligned multilayer samples of membranes containing gramicidin and ions (Tl^+ , K^+ , Ba^{++} , Mg^{++} or without ions). From the difference electron density profiles, we found a pair of symmetrically located ion binding sites for Tl^+ at $9.6 \pm 0.3 \text{ \AA}$ and for Ba^{++} at $13.0 \pm 0.2 \text{ \AA}$ from the midpoint of the gramicidin channel.

Gramicidin in the same conformation as defined by CD has been examined for its helical sense. It was first determined to be left-handed by ^{13}C NMR chemical shift measurements (Urry *et al.*, 1979; Urry, 1985), but a more recent 2-D ^1H -NMR study determined it to be right-handed (Arseniev *et al.*, 1985; see also Cornell *et al.*, 1988 and Nicholson & Cross, 1989). In either case, it is quite natural to suggest that the ion binding site is on the first turn of the helix from the mouth (Hladky & Haydon, 1984; Jordan, 1988). At the mouth of the channel, the last six carbonyls (D-Leu-10 to L-Trp-15) are hydrogen-bonded only to one neighbor; three unbonded carbonyl oxygens (Leu-10, 12, 14 in the case of a right-handed helix, Trp-11, 13, 15 in the case of a left-handed) are pointing toward the outside of the channel, as is the hydroxyl group of the ethanol amine tail. The surprising finding of our experiment is that the Tl^+ binding site, at $9.6 \pm 0.3 \text{ \AA}$ from the channel midpoint, is either near the bottom of or below the first turn of the helix (Koeppe & Kimura, 1984).

On the other hand, Ba^{++} ions, at $13.0 \pm 0.2 \text{ \AA}$ from the channel midpoint, apparently bind to the channel near the ends. This location is consistent with the experimental observation that divalent cations do not permeate but block the channel (Bamberg and Läuger, 1977). Thus we suggest that the separation between two opposite Ba^{++} binding sites, i.e., $26.0 \pm 0.4 \text{ \AA}$, is a good measure for the length of the gramicidin channel. The molecular basis for the selectivity against divalent cations is probably straightforward. The gramicidin channel is a pore of 4 \AA in diameter separated from the a hydrophobic dielectric medium only by a single layer of polypeptide backbone. A cation entering the channel must overcome its dehydration energy (Pullman, 1987) and encounters an image potential (Parsegian, 1969). Both the dehydration energy and the image potential are greater for divalent cations than for monovalent cations.

TRANSDUCTION OF NANOVOLT SIGNALS: LIMITS OF ELECTRIC-FIELD DETECTION

Life scientists of diverse backgrounds gathered in La Jolla, California, for three days in November 1989 to discuss the extreme electrical sensitivity of marine sharks, skates, and rays. The meetings were held at the Scripps Institution of Oceanography under the auspices of the Office of Naval Research, Igor Vodyanoy, Scientific Officer, Ad. J. Kalmijn, Convener.

After reviewing the results of earlier studies on the electric sense at the animal and system levels, the participants discussed the basic process of signal transduction in terms of voltage-sensitive ionic channels. Struck by the small charge displacements needed for excitation, they strongly recommended that sensory biologists, physiologists, and biophysicists join in a concerted effort to initiate new research on the ionic mechanisms of electric-field detection. To obtain detailed information on the electroreceptive membrane and its ionic channels, high-resolution recording techniques will be mandatory.

Marine elasmobranch fishes detect dc and low-frequency electric fields as weak as 5 nV/cm. The animals rely on their acute electric sense when homing in on the common bioelectric fields of prey, in orienting to the electric fields of ocean currents, and, perhaps, even in sensing their magnetic compass headings by detecting the fields they themselves induce when moving through the earth's magnetic field (Refs. 3, 4). Other, e.g., electrochemical and electrokinetic, fields may provide significant sensory cues as well.

The oceans' electric fields indeed present a wealth of sensory information. Nevertheless, as a group, apparently only the elasmobranch fishes have developed the sensory apparatus -- consisting of the ampullae of Lorenzini -- necessary to take full advantage of this sensory modality in the marine habitat. Scattered families of freshwater fishes either detect environmental electric fields that are about two orders of magnitude stronger, or they operate at higher frequencies in response to discharges of specialized electric organs.

The high electrical sensitivity of elasmobranch fishes is dictated by the low strengths, in terms of voltage gradients, of the signals in the oceans. The limits of electric-field detection are set by the noise per bandwidth of the sensory system and, ultimately, by the quantal nature of the ionic charge carriers. It is still uncertain, however, whether the transduction process is based on a refinement of familiar ion-channel kinetics, or whether the system functions in a different, more sophisticated manner.

The ampullae of Lorenzini are located in the head region. Each ampulla (Fig. 1) connects to the seawater by a jelly-filled canal, up to several centimeters in length, leading to a small pore in the skin. Important sources of noise are the receptor cells in the ampulla proper and the jelly of the ampullary canal. The thermal noise of the canal is coherent with regard to the receptor cells; the physiological noise of the individual receptor cells, however, is incoherent and may be reduced effectively by peripheral and central averaging. The noise of the many ampullary organs naturally is incoherent as well.

In addition to signal averaging, the animals may follow several strategies of active bandwidth reduction to enhance the relevant electrical signals and to suppress environmental and system noise. Sharks may need the full dc to 8 Hz system bandwidth to detect the steep, transient signals when approaching prey. In orientation, however, the signals resulting from the animals' swaying mode of locomotion through electric and magnetic fields are periodic. Since they are under direct control of the recipient animal, these signals lend themselves excellently to bandwidth reduction by coherent detection.

Moreover, the animals need not analyze the incoming signals in full detail to suppress noise but may focus on the salient stimulus features expected on the basis of former experience. In predation, for instance, the apparent rotation of the electric field with respect to the body axes during the early stages of the approach may offer less noisy sensory cues for guiding the animals to their targets than the weak intensity gradients of the source fields, although the intensity gradients may become more conspicuous and useful close to the source.

Notwithstanding the several strategies of noise suppression, it remains to be explained how the receptor-cell membrane detects threshold signals of 50 nV or less, calculated for environmental fields of 5 nV/cm known to elicit meaningful behavioral responses in small stingrays having their ampullary pores maximally 10 cm apart. Theoretically, a 50-nV threshold stimulus in the form of a step function yields a threshold current through the $8 \mu\text{m}^2$ apical membrane of each receptor cell (Fig. 2) of an estimated 12 electron charges per second.

The number of electronic charges needed to excite the receptor cells give direct hints as to the kinds and numbers of ionic channels involved (Ref. 2). At most two ionic channels per cell per second can be opened if each channel requires transmembrane transport of 6 gating charges, or four channels for 3 gating charges, etc. The channels that open must give rise to further depolarization of the apical membrane, perhaps in cooperation with the basal membrane of the receptor cell by positive feedback (Ref. 1). Since the ampullary nerve fibers are spontaneously active, no absolute threshold exists unless the system is limited by the quantal nature of the ionic charges.

The highest electrical sensitivity known in the Animal Kingdom demands full attention in its own right. Most excitable cells apparently operate at voltage levels sufficiently far from the limits of electric-field detection to be relatively insusceptible to the effects of noise and interference; conversely, other excitable cells may respond to lower electric-field levels than has been thought possible. Hence, man-made fields may be relatively harmless to most, but not to all cells, tissues, and organs of the human body.

The electroreceptive membranes also provide a unique opportunity for comparing the ionic mechanism of the animals versus the electronic mechanism of solid-state devices that have been adapted to detecting oceanic electric fields by use of ionic/electronic electrode interfaces. Operating near or, perhaps, at the limits of electric-field detection, marine sharks, skates, and rays set the Navy a real-life example of how to detect underwater objects at short range by sensing and appropriately processing their electric fields.

At the meetings, Charles S. Cox described the oceans' electric fields. Ad. J. Kalmijn, Carl D. Hopkins, and Harold H. Zakon reviewed the electric sense at the animal and system levels. Michael V. L. Bennett and William T. Clusin detailed the physiology of the receptor epithelia and sensory cells. Harvey M. Fishman and James C. Weaver discussed the electrical properties of excitable membranes. Maurice S. Montal and William F. Gilly considered the kinds of ionic channels likely to be involved. Leon J. Brunner and Charles N. Rafferty took an active part in the ensuing discussions. Robert Newburgh and Igor Vodyanoy outlined Navy needs. David W. Adelson served as the workshop secretary.

Ad. J. Kalmijn, Scripps Institution of Oceanography, La Jolla, CA 92093

References

1. Bennett, M.V.L. and Clusin, W.T. (1979). Transduction at electroreceptors: origin of sensitivity. In: Membrane Transduction Mechanisms. Cone, R.A. and Dowling, J.E. (eds.), Raven Press, New York, pp. 91-116.
2. Gilly, W.F. and Armstrong, C.M. (1984). Threshold channels -- a novel type of sodium channel in squid giant axon. *Nature*, 309:448-450.
3. Kalmijn, A.J. (1984). Theory of electromagnetic orientation: a further analysis. In: Comparative Physiology of Sensory Systems. Bolis, L., Keynes, R.D., and Maddrell, S.H.P. (eds.), Cambridge University Press, Cambridge, pp. 525-560.
4. Kalmijn, A.J. (1988). Detection of weak electric fields. In: Sensory Biology of Aquatic Animals. Atema, J., Fay, R.R., Popper, A.N., and Tavolga, W.N. (eds.), Springer-Verlag, New York, pp. 151-186.
5. Waltman, B. (1966). Electrical properties and fine structure of the ampullary canals of Lorenzini. *Acta Physiol. Scand.*, 66 (Suppl. 264):1-60.

Legends

Figure 1. Ampulla of Lorenzini. Ampullary canal (cut), sensory lobules of ampulla proper, and afferent nerve fibers. The walls of the lobules constitute the single-layered sensory epithelia, see Fig. 2. (After Waltman, Ref. 5.)

Figure 2. Sensory epithelium with pear-shaped receptor cells (clear) lodged between supporting cells (shaded). Each receptor cell has a true kinocilium (kc) protruding from the apical membrane into the ampullary jelly. The apical contacts between cells of the sensory epithelium feature tight junctions (tj). Afferent nerves form synapses (sn) at the basal membranes of the receptor cells. Sensory transduction takes place at the small apical membranes. The function of the kinocilium is unknown. (After Waltman, Ref. 5.)

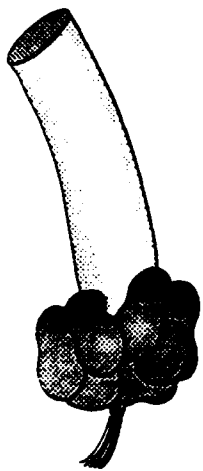


Fig.1

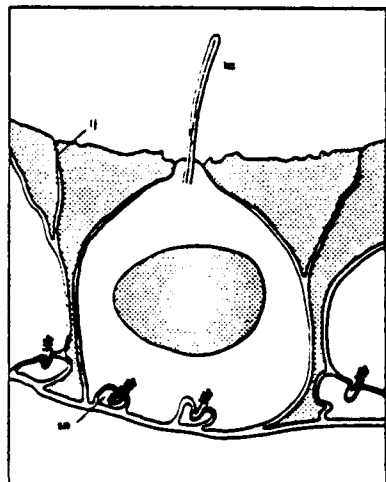


Fig.2

IMAGING MEMBRANE POTENTIAL ON NONEXCITABLE CELLS

Leslie M. Loew

Department of Physiology

University of Connecticut Health Center

Farmington, CT 06032, USA.

INTRODUCTION

This laboratory has recently developed 2 sets of potentiometric indicators which have been shown to be capable of reporting membrane potential in single cells (Gross et al., 1986; Ehrenberg et al., 1987; Ehrenberg et al., 1988; Gross and Loew, 1989). The structures and a summary of the properties of examples of each are depicted in the attached data sheets. This paper outlines several new imaging approaches which extend the utility of these dyes. Specifically, we will show that dual wavelength ratiometric measurements can be applied to the fast membrane staining dyes (Montana et al., 1989), and that simultaneous monitoring of plasma and mitochondrial membrane potentials is possible with the slow redistribution dyes via feature extraction and confocal microscopy (Farkas et al., 1989).

SIMULTANEOUS MEASUREMENT OF PLASMA AND MITOCHONDRIAL MEMBRANE POTENTIAL.

We have tested a series of highly fluorescent cationic redistribution dyes which have low membrane affinities and do not aggregate (Ehrenberg et al., 1988). Their distribution across the plasma membrane is governed primarily by the Nernst equation. Since the conditions of low self-association and low background binding to cellular components are met, the total fluorescence of cell suspensions containing these dyes is not sensitive to changes in membrane potential; however, after correction for a small amount of non-potential dependent binding, the ratio of the fluorescence intensity inside to that outside any particular cell corresponds to the Nernstian distribution of dye concentration, thus allowing determination of the membrane potential.

TMRE is one of the best behaved of these dyes in that it is rapidly and reversibly taken up by cells. It is, therefore, more suitable for dynamic and in situ quantitative measurements than the excellent mitochondrial stain rhodamine 123, which is a close structural analog. In a typical experiment, a digital video microscope is used to acquire a time series of fluorescence images of cells plated onto a coverslip in the presence of 0.1 μ M TMRE. The coverslip is placed on a microscope flow chamber so that the solutions bathing the cells can be easily exchanged. In this way, reagents which may perturb the permeability of the membrane or the metabolic activity of the mitochondria may be introduced and their effect on the dye distribution monitored. The more punctate regions of fluorescence within each cell are associated with the mitochondria. If only the plasma membrane permeability is affected, the mitochondrial fluorescence drops concertedly with that of the cytosol, as would be expected for a dye in a dynamic equilibrium between compartments held at differing electrical potentials, but the punctate pattern is maintained. This indicates that the plasma membrane potential is dropping, but the mitochondrial potential is being conserved. If both the plasma and mitochondrial membranes are permeabilized, fluorescence is lost from the entire cell. If a mitochondrial uncoupler is introduced, the contrast between the cytosolic and mitochondrial fluorescence is lost.

These cases can be analyzed and the kinetics estimated via digital image processing. Before any changes take place, an image of the cell is segmented according to the different intensity ranges corresponding to the mitochondrial and cytosolic regions. Thus, 2 templates are produced which can be used to analyze intensity variations within these regions in all subsequent images. Image sets and analyses representing all of these situations are included in a recent paper from our laboratory (Farkas et al., 1989). One example, in which the cell is treated with the uncoupler FCCP, is analyzed in Figure 1. As dye spills out of the mitochondria, there is actually a transient increase in cytosolic fluorescence. The punctate fluorescence characteristic of polarized mitochondria disappears and the cell becomes uniformly bright. Intensities from these regions are differentiated by the creation of binary templates from one of the

pre-FCCP images. These templates are produced interactively by setting high and low thresholds that highlight the respective regions within the cell. A single pair of templates is used to analyze fluorescence in all the images. Figure 1 also illustrates the equilibration time for accumulation of the dye - in these cells $t_{1/2} \approx 30s$.

Digital video imaging with a standard fluorescence microscope is suitable for following changes in membrane potential and differentially analyzing the effects of a membrane active agent on the plasma and mitochondrial membranes. It cannot, however, quantitate the potential difference across either of these membranes. This is because the conventional light microscope produces images with rather broad depths of field. Thus, the intensity measured from the cytosol contains contributions from fluorescence emanating from outside the cell. This problem can be overcome by using a microscope photometer with small pinholes at the conjugate image planes where the field and measuring diaphragms are normally situated (Ehrenberg et al., 1988), but these are purely intensity measurements with no spatial information content. The confocal microscope solves the depth of field problem by producing an image of a thin optical slice of a cell. We can use this feature of a confocal microscope to determine the potential difference across the inner mitochondrial membrane as well as the plasma membrane. The images produced show very distinct mitochondrial fluorescence even in rounded cells and the digitized fluorescence intensities from these regions can be analyzed (Farkas et al. 1989) In one such measurement, the ratio of intensities from the mitochondria, cytosol and extracellular medium are 4700:22:1, respectively. For a cell depolarized via a high K⁺ medium and valinomycin, the contrast is significantly lower and the corresponding intensity ratios are 15:3:1. These latter values can be used as correction factors for non-potential dependent binding (see Ehrenberg et al., 1988 for a description of this analysis) leading to potentials in the untreated cell of -150 mV and -52 mV for the mitochondrial and plasma membranes, respectively, relative to an extracellular ground. The plasma membrane potential is in good agreement with previous reports (Ehrenberg et al., 1988, and references cited therein), but the measurement of mitochondrial membrane potential from individual mitochondria inside a living cell is clearly unprecedentd. We feel, however, that the estimate should be considered a lower limit since not even confocal imaging may be able to extract fluorescence exclusively from a volume as small as the mitochondrion. We hope to be able to apply 3-D deconvolution algorithms to these data to further refine the intensity measurements. The major experimental problem, however, is the high laser intensities required in the current generation of laser scanning confocal microscopes. The resulting photobleaching and photodynamic damage limits not only our ability to obtain a full series of optical slices, but also precludes the substitution of confocal for conventional microscopy in the acquisition of time sequences.

DUAL WAVELENGTH RATIO METRIC MEASUREMENT OF MEMBRANE POTENTIAL

We have developed a series of fast potentiometric dyes that undergo a small spectral shift in response to voltage changes across a lipid bilayer membrane (Fluhler, et al., 1985) via a putative electrochromic mechanism (Loew, et al., 1978; Loew, et al., 1979). Among the best of these dyes is di-4-ANEPPS, with a spectral shift large enough to produce a 10%/100mV fluorescence change at the optimal combination of excitation and emission wavelengths. Since the dye fluorescence is extremely sensitive to environment (e.g. binding to membrane causes a 100 fold increase in fluorescence quantum yield) the emission intensity can never directly measure membrane potential and has been used primarily to monitor potential transients; i.e. the scope of its usefulness is similar to that of other fast dyes. But the spectral shift has never been fully exploited.

We have recently shown (Montana et al., 1989) that a dual wavelength ratiometric scheme, similar to that developed for cation measurements (Grynkiewicz et al., 1985; Tsien and Poenie, 1986; Rink et al., 1982), can be applied to membrane potential measurements with fast membrane staining dyes like di-4-ANEPPS. It simply takes advantage of the spectral shift associated with the dye's sensitivity to voltage. Excitation is alternated between the blue and red wings of the absorption band and the fluorescence resulting from one wavelength divided by the fluorescence excited by the other. This ratio is linearly related to membrane potential for both macroscopic preparations, such as lipid vesicles in a fluorometer cuvette, or microscopic preparations, such as single cells attached to a cover slip (Montana et al., 1989).

Results of an experiment which incorporates microscope imaging are shown in Figure 2. In this experiment, HeLa

cells on a glass coverslip are subjected to a uniform externally applied electric field. For a round cell, this induces a membrane potential which varies along the surface according to the cosine between the field direction and the membrane normal; thus, one hemisphere of the cell is hyperpolarized and the other is depolarized (see Gross et al., 1986, for details). This is a rather uncommon technique for producing a well controlled potential but is actually quite convenient in that it operates on all the cells in the sample and nicely highlights the ability of the dye to measure variations in potential along the cell surface. A series of images was obtained at different external field strengths with blue and green excitation for 4 round or nearly round cells. Intensities from the 2 excitation wavelengths were integrated over a small patch of membrane at the poles of the cells and the corresponding ratios plotted against the membrane potential in Figure 2. The data is fit to a straight line via linear regression analysis. The slope is 0.09 ratio units / 100 mV and the fit has a correlation coefficient of 0.99.

CONCLUSION

We have presented a brief overview of some new approaches toward combining improved potential-sensitive dyes with emerging microscope imaging technologies. The templating technique uncovers distinct patterns of fluorescence changes corresponding to how membrane-active agents affect the mitochondrial and plasma membrane potentials. Laser scanning confocal images offer the possibility of quantitating the membrane potential in individual mitochondria in a living cell. Dual wavelength ratiometric measurements of fast membrane staining dyes can map out the variations in potential along the surface of a cell. These approaches open new experimental possibilities for monitoring membrane potential at the microscopic level in non-excitable cells - measurements which have very rarely been previously attempted.

A major limitation that remains for application to neuronal systems, is that the temporal resolution of the apparatus is still too low to permit monitoring of events as fast as action potentials. For some experimental objectives this limitation can be ignored and video technology can serve beautifully (Kauer, 1988). In most case, however, the photodiode array, pioneered by L. B. Cohen, offers an acceptable compromise by sacrificing spatial resolution to attain fast data acquisition times.

ACKNOWLEDGEMENTS

I am pleased to acknowledge the work of Mei-de Wei, Daniel Farkas, and John Carson in developing the methods and obtaining the results. I am also grateful to David Gross and Watt Webb for many useful discussions. This work was supported by USPHS grants AI22106 and GM35063.

REFERENCES

- Ehrenberg B, Farkas DL, Fluhler EN, Lojewska Z, Loew LM (1987). Membrane potential induced by external electric field pulses can be followed with a potentiometric dye. *Biophys J* 55:833-837.
- Ehrenberg B, Montana J, Wei M-d, Wuskell JP, Loew LM (1988). Membrane potential can be determined in individual cells from the nernstian distribution of cationic dyes. *Biophys J* 53:785-794.
- Farkas DL, Wei M, Febbroriello P, Carson JH, Loew LM (1989). Simultaneous imaging of cell and mitochondrial membrane potentials. *Biophys J* 56:1053-1069.
- Fluhler E, Burnham VG, Loew LM (1985). Spectra, membrane binding and potentiometric responses of new charge shift probes. *Biochemistry* 24:5749-5755.
- Gross D, Loew LM (1989). Fluorescent indicators of membrane potential: microspectrofluorometry and imaging. In Wang Y, Taylor DL (eds): "Methods in Cell Biology," Vol. 30, New York: Academic Press, pp 193-218.
- Gross D, Loew LM, Webb WW (1986). Optical imaging of cell membrane potential. Changes induced by applied electric fields. *Biophys J* 50:339-348.
- Grynkiewicz G, Poenie M, Tsien RY (1985). A new generation of Ca^{2+} indicators with greatly improved fluorescence

- properties. *J Biol Chem* 260:3440-3450.
- Kauer JS (1988). Real-time imaging of evoked activity in local circuits of the salamander olfactory bulb. *Nature* 331:166-168.
- Loew LM, Bonneville GW, Surow J (1978). Charge shift optical probes of membrane potential. Theory. *Biochemistry* 17:4065-4071.
- Loew LM, Scully S, Simpson L, Waggoner AS (1979). Evidence for a charge-shift electrochromic mechanism in a probe of membrane potential. *Nature* 281:497-499.
- Montana V, Farkas DL, Loew LM (1989). Dual wavelength ratiometric measurements of membrane potential. *Biochemistry* 28:4536-4539.
- Rink TJ, Tsien RY, Pozzan T (1982). Cytoplasmic pH and free Mg²⁺ in lymphocytes. *J Cell Biology* 95:189-196.
- Tsien RY, Poenie M (1986). Fluorescence ratio imaging: a new window into intracellular ionic signaling. *TIBS*:450-455.

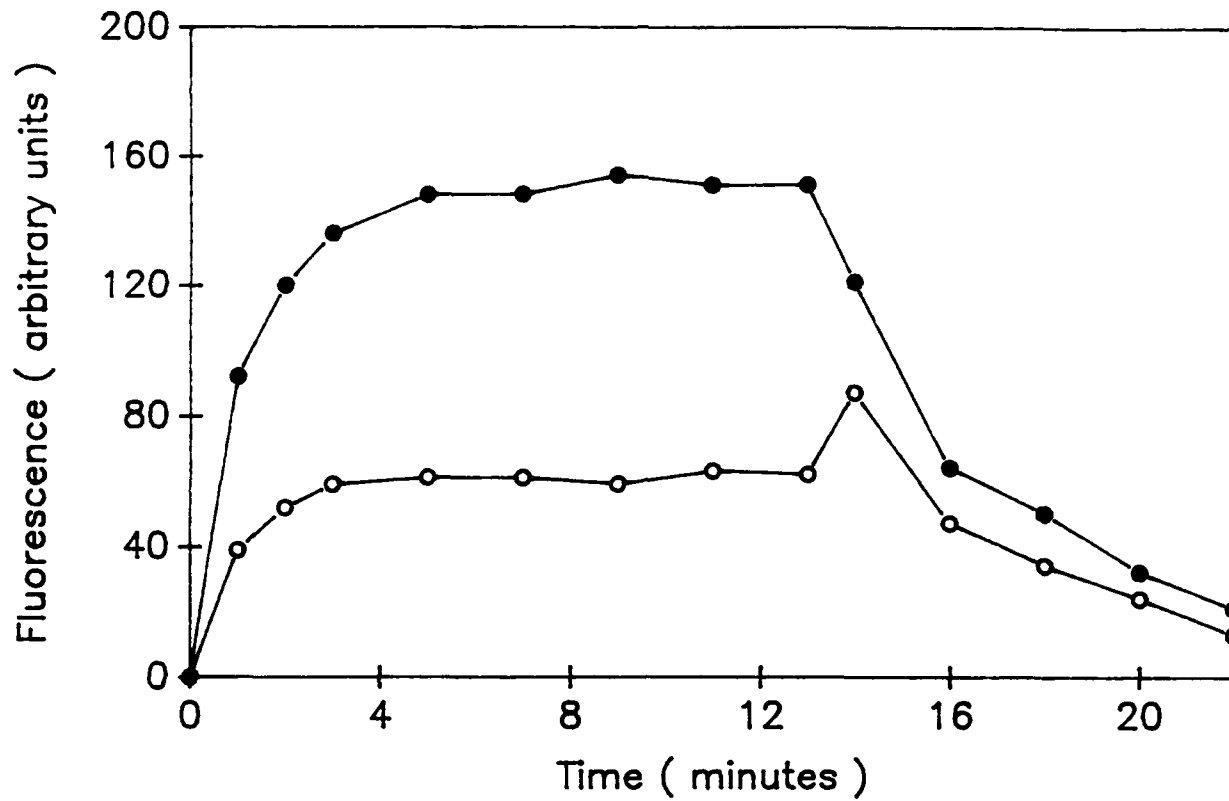


Figure 1. Fluorescence changes following treatment of TMRE-stained J774 cells with FCCP. At time 0, $0.1 \mu\text{M}$ TMRE is introduced and allowed to equilibrate with the cells. At 13 min $0.1 \mu\text{M}$ FCCP is introduced. Notice - mitochondrial fluorescence eventually merges with that of the cytosol.

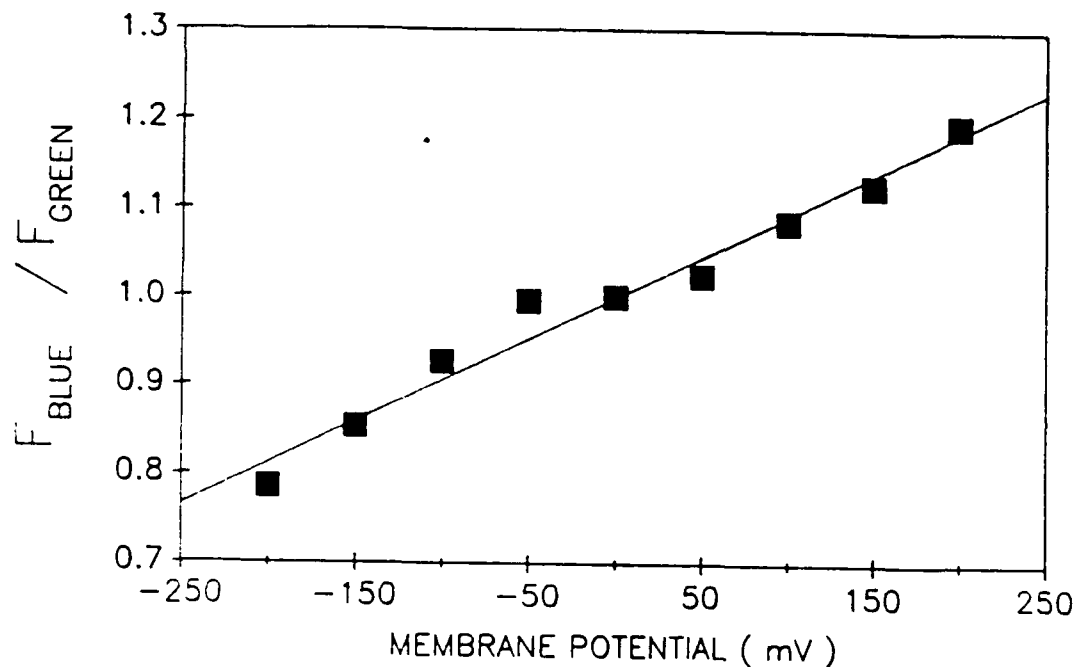


Figure 2. Ratios of intensities from excitation at 450 and 530 nm vs. membrane potential calculated from a solution to Laplace's equation for a spherical dielectric shell in a conducting medium. Data obtained from individual HeLa cells stained with di-4-ANEPPS at several applied field strengths. (reprinted from Montana et al., 1989)

Key to Potentiometric Probe Database

NAME - Name used most commonly in the Loew lab. JPW dyes were synthesized by Joe Wuskell. Most of the ASP and ANEP dyes were originally synthesized by Dov Birnbaum.

OTHER NAMES - Alternate names, especially those given by other labs. RH dyes were originally synthesized by Rena Hildesheim in Amiram Grinvald's Lab. RGA dyes were synthesized by Ravinder Gupta in Alan Waggoner's lab. WW dyes were originally synthesized by C.-H. Wang in the Waggoner lab. NK are commercially available from Nippon Kankoh Shikiso Kenkyusho Co., Ltd.

DESCRIPTION - The general chemical classification of the dye based on the molecular structure of the chromophore.

MW - Molecular weight.

CLASS - Fast \leq ms ; slow \geq s.

ABS PBS - Absorption maximum in aqueous solution, nm.

ABS ETOH - Abs max in ethanol.

ABS MEM - Abs max of dye in the presence of liposomes.

EM PBS - Emission maximum of an aqueous dye solution.

EM ETOH - Em max of dye in ethanol.

EM MEM - Em max of dye in the presence of liposomes.

FL INTENSITY - Weak: quantum yield < 0.005 ; strong > 0.1 .

REL TR/100 mV - Fractional change in transmitted light for a 100 mV voltage pulse across a spherical lipid bilayer membrane.

BEST ABS - Wavelength at which the transmitted light response is greatest on the spherical bilayer.

REL FL/100 mV - Fractional fluorescence change for a 100 mV potential pulse across a spherical lipid bilayer membrane.

BEST EX-EM - Excitation and emission wavelength combination with the best fluorescence change in the voltage clamped spherical bilayer.

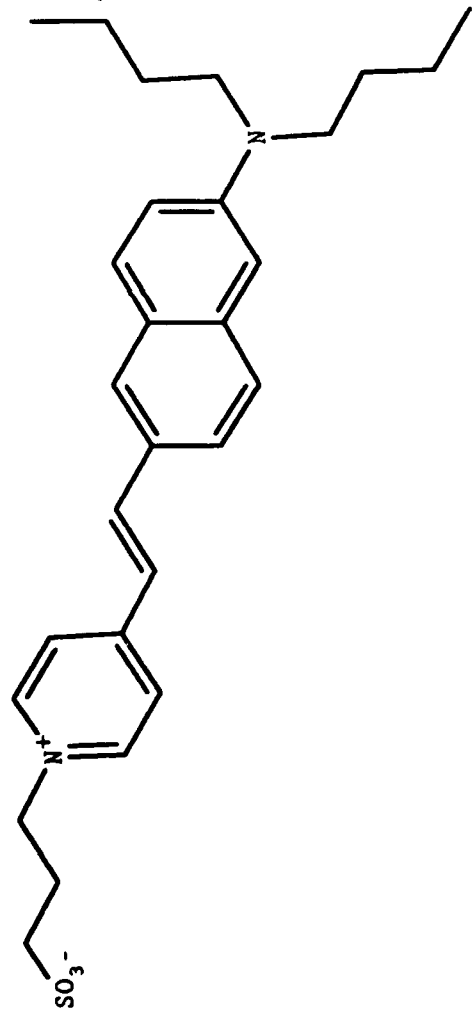
FL S/N SQ - Signal to noise for the fluorescence change with a 50 mV voltage pulse across a dye-stained squid giant axon.

ABS S/N SQ - Signal to noise ratio for the transmitted light change of a dye-stained voltage clamped squid axon.

AVAILABILITY - Quantity currently on hand.

COMMENTS - Usage, solubility, staining procedures, etc.

| | | | | | | | |
|-------------------|------------------------|--------------|---------------|--------------------|-------------------|---|--|
| TMRE | OTHER NAMES JPW-179 | MW 415.52 | CLASS SLOW | Abs ETOH nm 548 | EM ETOH nm 597 | | |
| | | | | Abs PBS nm 552 | EM PBS nm 596 | | |
| | | | | Abs MEM nm 559 | EM MEM nm 597 | | |
| | | | | Abs S/N SQ | FL S/N SQ | | |
| | | | | RelTr/100mV | RelFl/100mV | | |
| BEST EX-EM (nm) | BEST ABS (nm) | | FL INTENSITY | | | COMMENTS: | |
| | | | High | | | Redistribution dye for single cell measurements. Obtain from Molecular Probes, Inc. | |
| AVAILABILITY (mg) | DESCRIPTION | | | | | | |
| 200 | Rhodamine | | | | | | |

| DI-4-ANEPPS | OTHER NAMES JPW-211 | MW 480.67 | CLASS FAST | ABS ETOH nm 502 | EM ETOH nm 723 |
|---|------------------------|-------------------------|-----------------|--|-------------------|
|  | | | | | |
| BEST EX-EM (nm) | BEST ABS (nm) | FL INTENSITY | DESCRIPTION | COMMENTS: | |
| 545 - 670 | 515 | High for membrane bound | Naphthyl Styryl | Good initial choice. May need Pluronic to solubilize. Obtain from Molecular Probes, Inc. | |
| AVAILABILITY (mg) | 1500 | | | | |

HELICAL TRANSITIONS IN PEPTIDES AS POSSIBLE GATING MECHANISMS

Garland R. Marshall,* Denise D. Beusen, John D. Clark and Edward E. Hodgkin. Center for Molecular Design, Washington University, St. Louis, MO 63110 USA

The primary interest in peptaibol antibiotics, such as alamethicin, is related to their ability to induce voltage-dependent conductance changes in artificial bilayer membranes. The presence of α,α -dialkyl amino acids, such as α -methylalanine (MeA, aminoisobutyric acid, Aib), in these microbial natural products argues strongly for a special role related to function. One aspect is the conformational restrictions imposed by these amino acids. Despite the variety of conformations theoretically available to α,α -dialkyl amino acids, the impact of multiple substitutions of these amino acids on the overall conformation of a peptide is dramatic forcing of an α - or 3_{10} -helical conformation in most cases. The crystal structure of alamethicin, which contains eight MeA residues out of twenty, is predominantly α -helical, with NMR data supporting a similar solution conformation in methanol. According to our studies, those factors which govern helical preference include the inherent relative stability of the α -helix compared with the 3_{10} -helix, the extra hydrogen bond seen with 3_{10} -helices, and the enhanced electrostatic dipolar interaction of the 3_{10} -helix when packed in a crystalline lattice. The balance of these forces, when combined with the steric requirements of the amino acid sidechains, determines the relative stability of the two helical conformations under a given set of experimental conditions.

Transitions between the two helical forms may be responsible, in part, for the sensitivity to voltage seen with pores formed by peptaibol antibiotics, such as alamethicin. One motivation to consider the 3_{10} -helix is the activity of emerimicin on bilayers. Its length of 15 residues is insufficient to span the dielectric thickness of the membrane in the α -helical conformation ($15 \times 1.5 \text{ \AA}$ per residue = 22.5 \AA), while the 3_{10} -

helical conformation ($15 \times 2.0 \text{ \AA}$ per residue = 30 \AA) is sufficient. In natural ion channels, a bundle of four amphipathic α -helices has been suggested as a plausible structure for the pore-forming element of voltage-gated channels. Transition between the α - and 3_{10} -helix would change the relative orientation of sidechains at the channel interface, increasing the opposition of Lys and Arg sidechains which occurs at every third residues, and increase the diameter of the pore by electrostatic repulsion. This helical transition with the associated increase in length per residue of 0.5 \AA should also be considered as a possible transduction mechanism for transmembrane signaling in receptors which have a single transmembrane segment such as the insulin receptor.

In order to evaluate the feasibility of the 3_{10} -helix having a significant role in biological systems, we have determined the relative stability of model systems containing multiple α,α -dialkyl amino acids in the two helical conformations and determined the transitional energetics through molecular dynamics simulations. The energy differences between the α -helix and the 3_{10} -helix for decamers of MeA is the same order of magnitude as an additional hydrogen bond. The energetic transition barrier between the two helices is quite low suggesting that environmental effects, such as solvation, the external electric field and ligand binding, could trigger a conformational transition. While the presence of multiple MeA's decreases the energy difference between the α -helix and the 3_{10} -helix in peptaibol antibiotics and restrict the overall conformations to helical, similar transitions in membrane proteins could be responsible for transduction as the energy differences between helical types with normal amino acids are well within the range of environmental modulation.

Acknowledgement: This research was supported in part by National Institutes of Health grants GM24482 (GRM) and GM33918 (GRM).

Electrostatics, dimensionality, stoichiometry, cooperativity and the binding of basic amino acids in peptides and proteins to acidic phospholipids in membranes. Stuart McLaughlin, Jiyun Kim, and Marian Mosior. Dept. of Physiology & Biophysics, HSC, SUNY, Stony Brook, NY 11794. FAX 516-444-3432.

Phospholipid bilayers and monolayers have been used to test the Gouy-Chapman theory of the diffuse double layer. This theory predicts how the potential in the aqueous phase at the surface of a bilayer membrane depends on the surface charge density and monovalent salt concentration. Several different experimental techniques demonstrate the Gouy-Chapman theory, as modified by Stern to include ion adsorption, describes adequately the dependence of surface potential on charge density and salt concentration. The Gouy-Chapman theory also predicts how the potential should fall with distance from the surface: we have examined experimentally the profile of the potential. The theory assumes the charges on the surface are uniformly smeared over the interface; we examined experimentally the discreteness-of-charge effect on the adsorption of ions to charged bilayer membranes.

We are interested in the binding of small basic peptides to phospholipid bilayer membranes for two reasons. First, many intrinsic membrane proteins have clusters of basic residues on their cytoplasmic surfaces. Glycophorin provides a well studied example; 4 of the first 6 cytoplasmic residues after the single transmembrane region are positively charged. In a recent review Von Heijne (1990) concluded that "there is a strong correlation between the transmembrane topology of integral membrane proteins of all classes and the distribution of positively charged residues around the hydrophobic transmembrane regions." Furthermore, experiments from several different laboratories suggest that these clusters of positive charges play a major functional role and that "the difference in the charges of the 15 residues flanking the first internal signal-anchor determines its orientation, with the more positive portion facing the cytosol" (Hartmann et al., 1989). The mechanisms by which these clusters of positive residues help determine the orientation of the transmembrane proteins is not known. However, Hartmann et al. (1989) suggest that these positive residues might sense the local electric potential produced by negatively charged phospholipids, which are preferentially located on the cytoplasmic surface of the membrane. Thus we would like to know how regions of proteins containing clusters of positive charges distribute themselves in the electrostatic diffuse double layer adjacent to the membrane (McLaughlin, 1989) and how tightly these positive charges bind to the negative lipids. Second, we are interested in the binding of basic peptides to membranes because a number of cytoplasmic proteins bind to the negative lipid phosphatidylserine (PS) in both biological membranes and phospholipid bilayers. Protein kinase C is an important example (Nishizuka, 1988; Kikkawa et al., 1989; Parker et al., 1989). I will discuss the possibility that when the cluster of 5 basic residues on the putative pseudosubstrate site of PKC moves away from the 5 contiguous acidic residues on the putative substrate binding site, the basic residues can bind to acidic lipids on the cytoplasmic surface of the plasma membrane.

We measured the binding of Lys_n, Arg_n (n = 1-5) and a peptide identical to the pseudosubstrate region of PKC to phospholipid bilayer and monolayers. To investigate how the binding energies depend on the proximity of the lysine residues, we measured the binding of peptides with 5 lysine residues but with 1 or 2 alanine residues between each of the lysines. We studied the binding by making microelectrophoresis measurements on multilamellar vesicles, fluorescence measurements with the probe 2-(p-1-toluidinyl)naphthalene-6-sulfonate (TNS) on unilamellar vesicles, surface potential

measurements with an ionizing electrode positioned above a monolayer, and equilibrium dialysis measurements with large unilamellar vesicles.

Electrostatics, membranes, macromolecules

- Carnie, S., and S. McLaughlin. 1983. Large divalent cations and electrostatic potentials adjacent to membranes. *Biophys. J.* 44:325-332.
- Carnie, S. L., and G. M. Torrie. 1984. The statistical mechanics of the electrical double layer. *Adv. Chem. Phys.* 56:41-253.
- Langner, M., D. Cafiso, S. Marcelja, and S. McLaughlin. 1990. Electrostatics of phosphoinositide bilayer membranes: Theoretical and experimental results. *Biophys. J.* 57:335-349.
- McLaughlin, S. 1977. Electrostatic potentials at membrane-solution interfaces. *Curr. Top. Membr. Transp.* 9:71-144.
- McLaughlin, S. 1989. The electrostatic properties of membranes. *Annu. Rev. Biophys. Biophys. Chem.* 18:113-136
- Sharp, K., and Honig, B. 1990. Electrostatic interactions in macromolecules: theory and applications. *Annu. Rev. Biophys. Biophys. Chem.* 19:301-332.

Reviews of the calcium/phospholipid second messenger system

- Kikkawa, U., A. Kishimoto, and Y. Nishizuka. 1989. The protein kinase C family: heterogeneity and its implications. *Annu. Rev. Biochem.* 58:31-44.
- Nishizuka, Y. 1988. The molecular heterogeneity of protein kinase C and its implications for cellular regulation. *Nature (London)*. 334:661-665.
- Nishizuka, Y. 1989. Studies and prospectives of the protein kinase C family for cell regulation. *Cancer*. 63:1892-1903.
- Parker, P. J., G. Kour, R. M. Marais, F. Mitchell, C. Pears, D. Schaap, S. Stabel, and C. Webster. 1989. Protein kinase C -- a family affair. *Molecular and Cellular Endocrinology*. 65:1-11.

Clusters of basic residues on transmembrane proteins determine orientation

- Hartmann, E., T. A. Rapoport, and H. F. Lodish. 1989. Predicting the orientation of eukaryotic membrane-spanning regions. *Proc. Natl. Acad. Sci. USA*. 86:5786-5790.
- von Heijne, G. 1990. The signal peptide. *J. Membrane Biol.* 115:195-201.

Stoichiometry, cooperativity, dimensionality, Hill coefficients

- Adam, G., and M. Delbrück. 1968. Reduction of dimensionality in biological diffusion processes. In *Structural Chemistry & Molecular Biology*. A. Rich and N. Davidson, editors. W.H. Freeman & Co., San Francisco. 198-215.
- Berg, H. C. 1983. *Random Walks in Biology*. Princeton University press.
- Berg, H. C., and E. M. Purcell. 1977. Physics of chemoreception. *Biophys. J.* 20:193-219.
- Cantor, C. R., and P. R. Schimmel. 1980. *Biophysical Chemistry*. W. H. Freeman and Co., San Francisco. (see Chapter 15)
- Reynolds, J. A. 1979. Interaction of a divalent antibody with cell surface antigens. *Biochemistry*. 18:264-269.

SEVENTY WATER MOLECULES: UNRECOGNIZED ACTORS IN THE HEMOGLOBIN PLAY
Marcio F. Colombo, Donald Rau, Adrian Parsegian, NIADDK, National Institutes of Health, Bethesda, Maryland 20892, USA

The ability of proteins to perform the functions necessary for cellular vitality depends critically on an ability to regulate conformational states. Different structural states of biological macromolecules vary greatly in functional efficiency. Regulation of biological activity is frequently accomplished through the control of the equilibrium between these states. Several kinds of conformational transitions can occur, from small displacements of amino acid tilt, to large changes in configuration or polymerization state of subunits. Intrinsic to these conformational changes are changes in the organization of water associated with the proteins, reflecting changes in accessible solvent surface area and in protein-bounded cavity volume. There exist effectors that are capable of regulating the equilibrium between these structural states. Despite water being the most abundant molecule in the cell and despite the water content of proteins being subject to change accompanying conformational changes, little attention is given to its role as a regulator of biologically active conformations.

Results from this laboratory have previously shown that the equilibrium between open/closed channels is sensitive to water activity, or osmotic pressure. These results are most easily viewed as the osmotic work done to change the water volume of the protein bounded channel from open to closed state. Martin Blank has convincingly argued that there is a parallel between channel gating conformational changes and those that govern the oxygen loading of hemoglobin. The logic guiding these arguments is based on the Gibbs adsorption isotherm and the Gibbs/Duhem equation to connect the free energy of different conformational states with the adsorption of several ligands.

In this work, we show how a change in the water activity of the solution will alter the equilibrium between two protein conformations of hemoglobin with two different water accessible surface areas.

Recall that hemoglobin is a tetrameric macromolecule that binds oxygen reversibly and cooperatively. Its cooperativity results from

differences in O_2 affinity between two allosteric conformers. The MCW model, based on this, with a T conformer with low affinity for O_2 and R high one, provide a theoretical framework to describe the oxygenation of Hb. X-Ray diffraction studies of Hb have shown two distinct structures between deoxygenated (T) and oxygenated (R) states of this protein. Moreover, the oxygen binding properties of Hb are affected by the binding of several non oxygen ligands at non-oxygen binding sites, like 2,3-DPG, H^+ , Cl^- and CO_2 , which trigger heterotropic interactions responsible for the physiological control of the protein activity.

The oxygenation of normal Hb, stripped of inorganic phosphates and ions, had been investigated measuring the partial oxygen saturation as a function of oxygen pressure, in buffered solutions with different water activities. To control water activity, we have used several different and chemically distinct molecules, sucrose, stachyose, polyethylene-glycol 150, polyethylene-glycol 400 and glycerol. In solutions with different concentrations of these solutes, we observed that the affinity of Hb decreases with the rising of solutes concentrations, i.e., with the decreasing of water activity in the range studied, up to the osmotic pressure corresponding to about 50 atmospheres.

The data obtained have been analyzed via on the Gibbs-Duhem equation, assuming no interaction between cosolvent and Hb. Since we assume that the only two chemical components interacting with the protein are oxygen and water molecules this equation is expressed as,

$$n_{O_2} d\mu_{O_2} + n_w d\mu_w = 0 \quad (1)$$

where n_{O_2} and n_w are the number of oxygen and water, respectively, bound to the Hb and μ_{O_2} and μ_w the chemical potential of oxygen and water. By cross differentiation we obtain

$$(\delta n_{O_2} / \delta \mu_w)_{\mu_{O_2}} = (\delta n_w / \delta \mu_{O_2})_{\mu_w} \quad (2)$$

This relates the change in the oxygen saturation of Hb with the change in the water activity at constant oxygen pressure to the change

in the number of bound waters to the protein with the change in the oxygen activity at constant water activity.

The left term of equation (2) was obtained plotting the partial oxygen saturation at one oxygen pressure as a function of water activity. Doing this procedure for the whole oxygen loading curve, we could integrate these quantities as a function of the oxygen pressure to get the numbers of waters which is bound in excess to the Hb when it change its conformation from the deoxy to the fully oxygenated state.

Consistently, we found that approximately 70 water molecules bound to Hb upon going from deoxy to oxy form. This number is independent of the nature of the solute used, showing that the assumption of no interaction between cosolvent and protein is correct. Therefore, the effect of water activity on the oxygen affinity can be rationalized only considering the linkage between oxygen binding with the change in the protein hydration that follow the structural transition from T (deoxy) to R (oxy) structure upon oxygenation.

These results show that is possible to determine the number the water molecules linked with conformational transitions of native proteins by following the effect of water activity on the functional properties of these proteins and point out the possibility of using osmotic experiments to test models of protein activity in which changes in the conformation are assumed to occur.

THEORETICAL INVESTIGATION OF DNA TRANSLOCATION THROUGH THE CELL
MEMBRANE

V.Ph.Pastushenko

The A.N.Frumkin Institute of Electrochemistry of the USSR
Academy of Sciences, Moscow V-71, Leninsky prospekt 31.

Like in electroporation and electrofusion of cells EF plays essential role in translocation of DNA through the cell membrane in electrotransformation experiments. Several questions are important for theoretical elucidation of the mechanism of DNA translocation: 1) how many molecules penetrate into the cell during electric pulse; 2) do the DNA molecules penetrate through membrane pores freely due to electrophoresis or essential interaction between the molecules and the cell membrane takes place; 3) is the interaction between DNA and membrane strong enough to cause the increase of pore size or membrane invagination? To answer these questions one should know 1) the permeabilized state of the cell membrane, i.e. size and distribution of pores at cell poles; 2) the distribution of EF around the cell permeabilized by strong pulse of EF; 3) the behaviour of DNA approaching the pore; 4) the forces exerted on the cell membrane due to its interaction with DNA molecule.

Assuming that the membrane conductivity at cell poles is known we find theoretically the EF distribution inside and around the cell. The volume of reaction zone (region from which the molecules reach the permeabilized portion of the membrane during EF pulse) can be directly calculated basing on this distribution and neglecting dependence of electrophoretic mobility on DNA conformation and orientation. Multiplied by DNA

concentration this volume enables the upper estimation of the number of molecules penetrating into the cell during one EF pulse.

The molecular orientation is favored by inhomogeneity of EF which increases the probability that the molecule enters the pore normally to the membrane surface and penetrates into the cell electrophoretically. The force of interaction between the molecule free to move electrophoretically through the pore and pore walls is estimated; this force decreases exponentially with increase of the pore radius, characteristic length is the Debye - Huckel radius. The force increases essentially if the molecule moves slowly through the pore due to its steric interaction (of different nature) with the membrane.

If nonoriented molecule approaches the pore its penetration into the cell is possible if the molecule or the membrane suffer deformation. The forces characterizing the molecule/membrane interaction and necessary for molecule/membrane deformation are discussed and estimated theoretically. The possibility of the field induced membrane invagination and formation of vesicle containing DNA is discussed.

MEMBRANE CURVATURE, LIPID SEGREGATION, AND STRUCTURAL TRANSITIONS FOR
PHOSPHOLIPIDS UNDER DUAL SOLVENT STRESS

R. P. RAND^{*} and N. L. FULLER, Brock University; M. GRUNER, Princeton University; V. A. PARSEGIAN, National Institutes of Health.

ABSTRACT (From Biochemistry 29:76, 1990)

Amphiphiles respond both to polar and non-polar solvents. In this paper X-ray diffraction and osmotic stress have been used to examine the phase behavior, structural dimensions, and the work of deforming the monolayer-lined aqueous cavities formed by mixtures of dioeoylphosphatidylethanolamine (DOPE) and dioeoylphosphatidylcholine (DOPC) as a function of concentration of the two solvents, water and tetradecane (td). In the absence of td, most PE/PC mixtures show only lamellar phases in excess water; all of these become single reverse hexagonal (H_{II}) phases with addition of excess td. The spontaneous radius of curvature, R_0 , of lipid monolayers, as expressed in these H_{II} phases, is allowed by the relief of hydrocarbon chain stress by td; R_0 increases with the ratio of DOPC/DOPE. Mixtures with very large R_0 's can have water contents higher than the $L\alpha$ phases that form in the absence of td. The drive for hydration is understood in terms of curvature energy to create large water cavities in addition to direct hydration of the polar groups. Much of the work of removing water to create hexagonal phases of radius $R < R_0$, goes into changing monolayer curvature rather than dehydrating polar groups.

Single H_{II} phases stressed by limited water or td, show several responses. (a) The molecular area is compressed at the polar end of the molecule and expanded at the hydrocarbon ends. (b) For circularly symmetrical water cylinders, the degree of hydrocarbon chain splaying and polar group compression are different for molecules aligned in different directions around the water cylinder. (c) A pivotal position exists along the length of the phospholipid molecule where little area change occurs as the monolayer is bent to increasing curvatures. (d) By defining R_0 at the pivotal position, we find that measured energies are well fit by a quadratic bending energy $K_0/2(1/R - 1/R_0)$; the fit yields bilayer bending moduli of $K_C = 1.2 - 1.7 \cdot 10^{-12}$ ergs, in good agreement with measurements from bilayer mechanics. (e) For lipid mixtures, enforced deviation of the H_{II} monolayer from R_0 is sufficiently powerful to cause demixing of the phospholipids in a way suggesting that the DOPE/DOPC ratio self-adjusts so that its R_0 matches the amount of td or water available, and that curvature energy is minimized.

VARIATION IN HYDRATION FORCES BETWEEN NEUTRAL PHOSPHOLIPID BILAYERS. EVIDENCE FOR HYDRATION ATTRACTION.

R. P. RAND and NOLA FULLER, Brock University, V. A. PARSEGIAN and D. C. RAU, National Institutes of Health.

ABSTRACT (From Biochemistry 27:7711, 1988)

It is now generally recognized that hydration forces dominate close interactions of lipid hydrophilic surfaces. The commonality of their characteristics have been reasonably established. However differences in measured net repulsion, particularly evident when comparing phosphatidylethanolamine (PE) and phosphatidylcholine (PC) bilayers, suggest there exists a variety of behavior wider than expected from earlier models of hydration and fluctuation repulsion balanced by van der Waals attraction. To find a basis for this diverse behavior we have looked more closely at measured structural parameters, degrees of hydration and interbilayer repulsive forces for the lamellar phases of the following lipids: 1-palmitoyl-2-oleoyl-PE (POPE), egg PE, transphosphatidylated egg PE (egg PE-T), mono- and di- methylated egg PE-T, (MMPE and DMPE), 1-stearoyl-2-oleoyl-PC (SOPC), and mixtures of POPE and SOPC. POPE and SOPC bilayers differ not only in their maximum degrees of hydration but also in the empirical hydration force coefficients and decay lengths that characterize their interaction. When mixed with POPE, SOPC effects sudden and disproportionate increases in hydration. POPE, egg PE and eggPE-T differ in their degree of hydration, molecular area and hydration repulsion. A single methylation of eggPE-T almost completely converts its hydration and bilayer repulsive properties to that of egg PC; little progression of hydration is seen with successive methylations. In order to reconcile these observations with the conventional scheme of balancing interbilayer hydration and fluctuation-enhanced repulsion with van der Waals attraction, it is necessary to relinquish the fundamental idea that the decay of hydration forces is a constant determined by the properties of the aqueous medium. Alternatively one can retain that fundamental idea if one recognizes the possibility that polar group hydration has an attractive component to it. In the latter view, that attractive component originates from interbilayer hydrogen-bonded water bridges between apposing bilayer surfaces, arising from correlation of zwitterionic or other complementary polar groups or from factors that affect polar group solubility. We suggest that the full range of degrees of hydration and of interbilayer spacings observed for different neutral bilayers results in part from variable contributions of the attractive and repulsive hydration components. The extremes are exemplified by the dominance of attraction between PE bilayers with crystalline hydrocarbon chains and the dominance of repulsion and full hydration of melted PC bilayers. Within the variable hydration of the PE's with melted chains, one sees evidence of variable hydration attraction. With or without the postulated attraction though, good estimates of adhesion energy can be obtained. It is necessary therefore to make other critical tests to distinguish the alternatives.

EFFECTS OF NEUTRAL LIPIDS ON DIVALENT - CATION - INDUCED INTERACTIONS BETWEEN
PHOSPHATIDYL SERINE-CONTAINING BILAYER MEMBRANES

R. P. RAND and J. COORSSEN, Brock University, St. Catharines, Ontario, Canada.

ABSTRACT (From Studia Biophysica 127:53, 1988)

Interactions between all phospholipid membranes near contact are dominated by a strong hydration repulsive force resulting from the work of removing water from the hydrophilic polar groups. One widely used method capable of overcoming this force and enhancing contact is by triggering the interaction of bilayers made of acidic phospholipids with divalent cations. Such interactions can produce adhesion energies so strong that the bilayers undergo major structural changes and near-complete dehydration. This is accompanied by the destruction of vesicular systems, the expulsion of enclosed aqueous contents and the formation of condensed multilamellar structures. Increasing the neutral lipid content of such bilayers decreases the energy of contact but often results in the separation of the different lipid components into two different regions. It is often difficult to distinguish whether those two regions are within each bilayer, lateral segregation, or are separated from each other, bulk segregation. Such a distinction is important in the context of bilayer contact since lateral segregation requires a reconciliation of hydration forces of the different lipids, while bulk segregation would allow each lipid to express its own hydration properties. Indeed we have argued that different hydration energies can be expected to drive lipid segregation when mixed lipid bilayers are forced together. We have investigated in some detail the structure of the Ca-induced contacts formed between bilayers containing dioleoyl-phosphatidylserine (PS) and -choline (PC) over the entire range of mixtures. X-ray diffraction, freeze-fracture electron microscopy, density gradient centrifugation and osmotic stress methods were applied to the structures formed after triggering the interaction of unilamellar bilayer vesicles. From 100 to ~ 50 mole % PS, the contact is nearly completely dehydrated. Importantly, even with one of the polar groups most difficult to dehydrate, all the PC is found in the contact region. This PC must be near-fully dehydrated, the energy for which must come from the formation of a Ca-PS complex. For increasing PC contents above 50 mole% there is a systematic increase in the interbilayer distance and PC remains in the contact region. The lipids in this more hydrated contact however are susceptible to bulk segregation into lamellar phases resembling the pure components.

CONFORMATIONAL DYNAMICS AND ELECTRON TRANSFER (E_1)
IN PHOTOSYNTHETIC MEMBRANE PROTEINS

Andrew B. Rubin

Moscow State University, Department of Biophysics

Electron transport through the photosynthetic electron chain is accompanied by generation of local electric fields. The upset of equilibrium in the distribution of the ions leads to the generation of a transmembrane electrochemical gradient, an energy store utilized for ATP synthesis. Following the primary charge separation within the protein of the photoactive reaction center (RC) of purple bacteria, an electron is transferred for 5-6 ps through intermediate electron carriers (bacteriopheophytin) causing reduction of the secondary quinone for about 100 ms. The electron transfers within the reaction centers occur even at low temperatures, suggesting that the transfer of an electron is by tunneling. The problem is to elucidate the involvement of the structural components of the photosynthetic membrane and photoactive reaction center protein in the above process.

By radioscopy techniques (ESR, gamma-resonance spectroscopy) it has been found that conformational mobility of the reaction center protein increases over the temperature range (250-200 K) within which the functional activity of electron transfer from the primary to secondary quinone ($Q_A \rightarrow Q_B$) was seen to increase. In dehydrated RC preparations which loose functional activity and in chromatophore films of purple bacteria, increasing the preparation hydration caused a recovery of functional activity simultaneously with activation of intramolecular motions within the hydration range.

(relative values of 0.2 to 0.3 P/P_0) where the primary hydration shell is formed over the reaction center protein. Using NMR spectroscopy and varying the hydration of the preparation, we monitored the mobility of the components of the photosynthetic membrane by measuring spin-lattice (T_1) and spin-spin (T_2) relaxation times of the H_2^{31} and C^{13} nuclei of the hydration water. It appeared that the acceleration of electron transfer through the $Q_A \rightarrow Q_B$ pathway at $P/P_0 \sim 0.3$ was accompanied by a more intense rotational motion of the hydrocarbon moiety in the hydrophobic region of the membrane. When the oxidation of cytochrome c by photoactive pigment P^+ occurs at a faster rate, the protein and lipids show much more mobility at high hydration ($P/P_0 \sim 0.7$). The cause of this is large-scale structural rearrangements that the membrane proteins, cytochrome and reaction center undergo in attaining the appropriate mutual orientation. In the paper, models of intramolecular conformational mobility of the membrane-associated proteins are discussed based on motions of enzymes in heavily viscous medium. In the system under consideration, a sharp retardation of intramolecular motions is observed along some degrees of freedom at low temperature. The transfer of an electron to the acceptor moiety and generation of local electric fields result in a polarization of the nearest protein surrounding and its structural/conformational rearrangement.

We conducted experiments on chromatophore preparations from purple bacteria and investigated low-temperature reactions of quinones after freezing the samples in the dark and light. In samples frozen in the light, the primary quinone is reduced (Q_A^-). Due to the polarization and rearrangement within the protein carrier in this case, quinone Q_A^- is shifted from P^+ toward Q_B .

by as large as 1 \AA . This provides a condition for a directional transfer of the electron to occur. The rate of the Q_A to C_B electron transfer at 77 K was smaller in the dark-frozen sample, as compared with that for the sample frozen in the light (10^3 s^{-1}) to the same temperature. A reverse relationship of the rates holds for the back return of the electron from Q_A to P^+ (5 s^{-1} in the dark and 1 s^{-1} in the light). Applied electric field may influence the polarization-induced rearrangements in the protein. This was seen as field-induced (10^7 V m^{-1}) spectral changes in the photosynthetic membranes (absorption changes in the spectral region where carotenoids absorb; rise of delayed luminescence). In experiments using air-dried films of purple membrane we observed that in applied electric field ($\sim 10^7 \text{ V m}^{-1}$) the photointermediate M_{412} of the bacteriorhodopsin photoreaction cycle decays more slowly. Electric field applied to such films in the dark at room temperature caused absorption changes, indicating the formation of the batho-BR(K) form of the first photointermediate of the BR₅₇₀ photocycle. Under these conditions, the polarization effects of applied electric field cause a proton displacement about the Schiff base, and also affect the proton translocation through the proton-pumping channels.

REFERENCES

1. Rubin A.B., Kononenko A.A., et al., "Polarization effects on photosynthetic membranes", International Journal of Quantum Chemistry, XYII, 587-593, (1980).
2. Krupyanskii Yu.P. et al., "The mobility of chromatophore membranes from *Ec.t.shaposhnikovii* revealed by Rayleigh scattering of Mossbauer radiation (RSMR) experiments", Sur.Biophys.J., 12, 107-114 (1985)

3. Rubin A.B., Shaitan K.V., Kononenko A.A., Chamorovsky S.K.,
"Temperature dependence of cytochrome photooxidation and
conformational dynamics of Chromatium reaction center complexes",
Photosynthetic Research, 22, 219-231 (1989).

**Ion Transport Across Excitable Cell Membranes
Measured with Tracers**

R. A. Sjodin, J. G. Montes, and Y. Wu

Outline of Presentation

1. Brief Background for Ion Transport Studies
2. Recent Work on Mg Ion Regulation
3. Use of Stable Isotopes as Tracers by Mass Spectrometry
4. Our Recent Entry into Electrofusion Research

Simultaneous bidirectional magnesium ion flux measurements in single barnacle muscle cells by mass spectrometry

Joseph G. Montes, Raymond A. Sjodin, Alfred L. Yerger,* and Nancy E. Vieira*

Department of Biophysics, University of Maryland School of Medicine, Baltimore, Maryland 21201; and *Laboratory of Theoretical and Physical Biology, National Institute of Child Health and Human Development, National Institutes of Health, Bethesda, Maryland 20892

ABSTRACT Stable isotopes of Mg were used to measure bidirectional magnesium ion fluxes in single barnacle giant muscle fibers immersed in Ca- and Na-free, isosmotic media. Measurements were made using a mass spectrometric technique, thermal ionization mass spectrometry (TIMS), in conjunction with atomic absorption spectroscopy. Kinetic relations based on a first-order model were developed that permit the determination of unidirectional rate coefficients for Mg influx, k_{in} , and efflux, k_{out} , in the same experiment from knowledge of initial conditions and the initial and final ratios of $^{28}\text{Mg}/^{24}\text{Mg}$ and $^{25}\text{Mg}/^{24}\text{Mg}$ in ambient solutions (i.e., by isotope dilution). Such determinations were made for three

values of the external Mg ion concentration: 5, 25, and 60 mM. At the concentration $[\text{Mg}^{+2}]_o = 5 \text{ mM}$, k_{in} and k_{out} were about equal at a value of 0.01 min^{-1} . At the higher values of $[\text{Mg}^{+2}]_o$, the values of k_{in} increased along a curve suggesting saturation, whereas the values of k_{out} remained essentially constant. As could be expected on the basis of a constant k_{out} , the initial influx rate varied in direct linear proportion to $[\text{Mg}^{+2}]_o$, and was $11.3 \text{ pmol/cm}^2\text{s}$ when $[\text{Mg}^{+2}]_o$ was 5 mM . However, the initial efflux rate appeared to increase nonlinearly with $[\text{Mg}^{+2}]_o$, varying from $\sim 3.4 \text{ pmol/cm}^2\text{s}$ ($[\text{Mg}^{+2}]_o = 5 \text{ mM}$) to $\sim 80 \text{ pmol/cm}^2\text{s}$ ($[\text{Mg}^{+2}]_o = 60 \text{ mM}$). The results are consistent with a model that assumes Mg influx to be mainly an

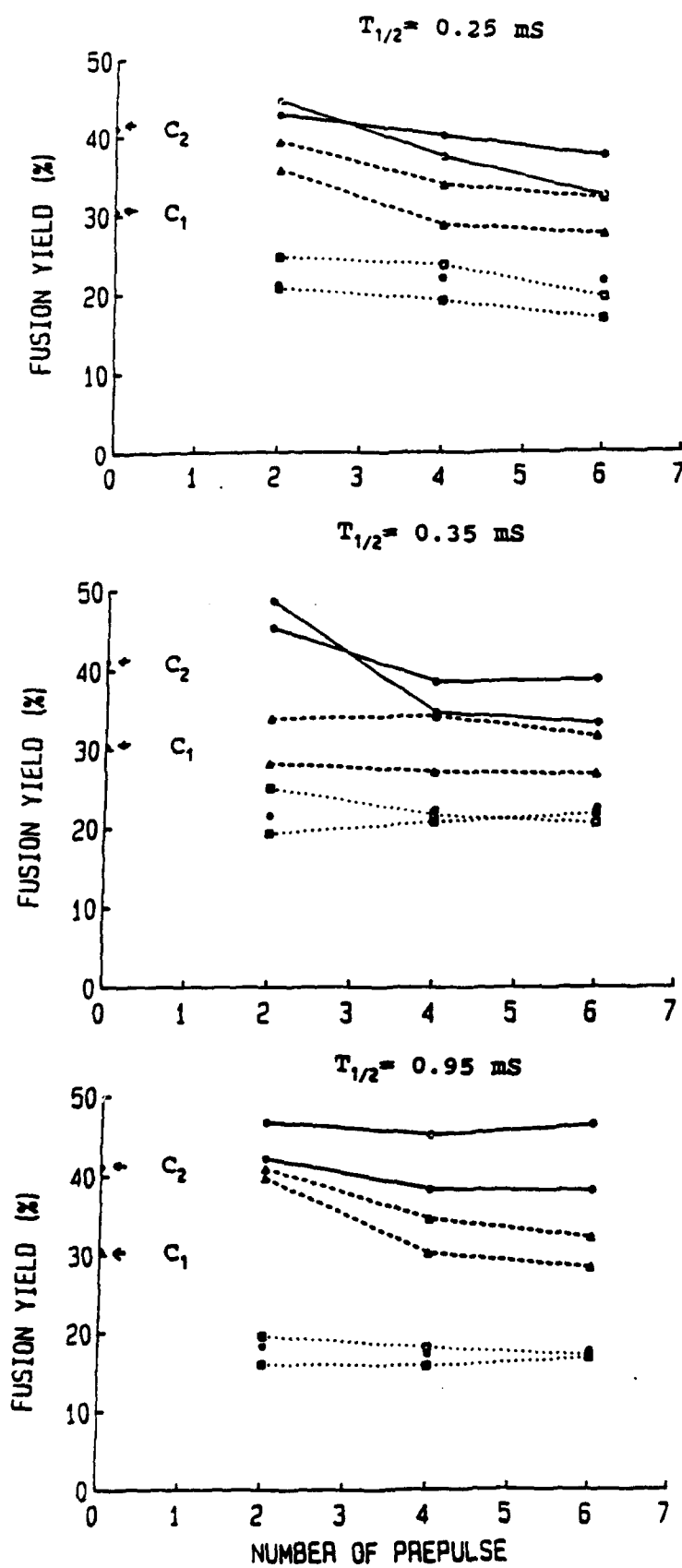
electrodiffusive inward leak with $P_{\text{Mg}} = 0.07 \text{ cm/s}$ and Mg efflux to be almost entirely by active transport processes. Where comparisons can be made, the rate coefficients determined from stable isotope measurements agree with those previously obtained using radioactive Mg. The rate coefficients can be used to correctly predict time-dependent changes in total fiber Mg content. The results support the conclusion that nonradioactive tracers can be used to measure ion fluxes and ion flux ratios in excitable cells. It is expected that this method will greatly assist in the study of Mg regulation in general.

THE ADDITIVITY OF PULSE ENERGY AND THE ROLE OF THE ELECTRIC FIELD STRENGTH IN THE ELECTROFUSION OF RABBIT ERYTHROCYTE GHOSTS

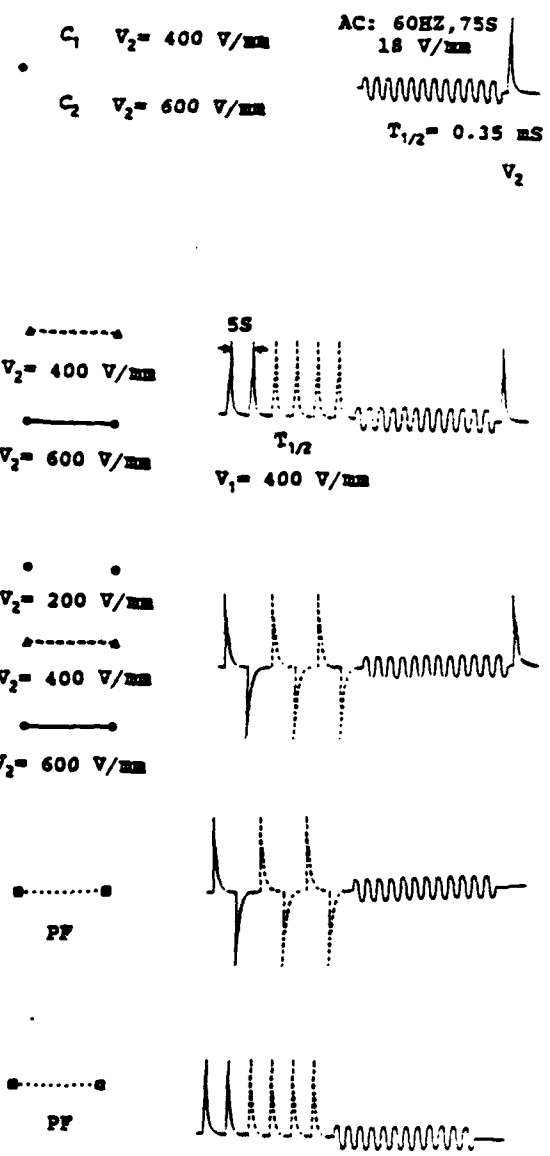
Raymond A. Sjodin, Yankuan Wu, and Joseph G. Montes
Department of Biophysics, School of Medicine,
University of Maryland at Baltimore, Baltimore, MD 21201

ABSTRACT

Electrically induced membrane fusion can be produced in two ways. One is the usual electrofusion protocol (CF protocol). The other means is the reverse process of the CF protocol, that relying on the so-called "long-lived fusogenic state" (PF protocol). The mechanistic hypotheses for the fusion states produced by the PF protocol fall into two categories: electropore hypotheses and point-defect hypotheses. To study the relationship between the long-lived fusogenic state and the "usual" electrofusion state and the possible mechanisms of membrane fusion, fusion yield for rabbit erythrocyte ghosts was determined using a "PF-CF" protocol, whereupon ghosts are first treated with a train of prepulses of the same electrical characteristics and then immediately subjected to a typical CF protocol. The polarity of the prepulses in a train can be either the same or it can be varied. In our studies, experiments were conducted in a suspension of low cell population density (10^7 cells/ml) in a 20-mM sodium phosphate buffer (pH 8.5). Fusion yields were measured using Dil as the fluorescent label. The detailed experimental protocols and results are on the following page. Fusion yields were generally not increased with an increase in the number of prepulses beyond two; instead, a small decrease in the yields was typically observed. Nonetheless, fusion yields were still increased by using a couple of prepulses which have the same or alternative polarities before applying the final pulse. This effect may be due to an increase in cell sphericity which allows cells to make a larger zone of contact with each other following the prepulses; the general decline in fusion yield observed with a further increase in the number of prepulses may be a consequence of a reduction in the percentage of cells that aggregate into pearl chains under those conditions (data not shown). When the electric field strength of the prepulses was equal to or lower than that of the final pulse, fusion yields were close to those for the CF protocol; however, they were closer to those for the PF protocol when the strength of the prepulses was higher than that of the final pulse. It was evident that the CF protocol for cell fusion was more efficient than the PF protocol. Varying the decay half-time ($T_{1/2}$) (i.e., the power) of the prepulses had little or no effect on the fusion yields in most of the experiments, indicating that changing the electric field strength is the major way to increase the fusion yield. The results clearly show that the effect on membrane fusion yield of the electric energy delivered by the pulses is not additive, but rather suggests saturability of the long-lived fusogenic state and possible identity of that state with the state occurring with the usual electrofusion protocol, at least under certain conditions. Since the effect of electric pulses on the cell membrane could conceivably be reversible, we performed experiments whose purpose it was to "erase" the "memory" of previously applied prepulses by immediately following the prepulses with prepulses of the same energy but opposite polarity. There was no significant difference in fusion yield whether the polarity of prepulses was alternated or not. These results appear to favor an electropore hypothesis rather than a point-defect hypothesis, and suggest that the mechanism for both the long-lived fusogenic state and the usual electrofusion state may be the same.



SCHEMATIC REPRESENTATION OF EXPERIMENTAL PROTOCOLS FOR THE THREE GRAPHS AT LEFT



REFERENCES

- Bates, G., Saunders, J., and Sowers, A.E., 1987, Electrofusion: Principles and applications, in: *Cell Fusion* (A.E. Sowers, ed.), Plenum Press, New York, pp.367-395.
- Chernomordik, L.V., Sukharev, I.G., and Abidor, I.G., 1985, Long-living defects in BLM after reversible electrical breakdown, *Biol. Membr.* 2:87-94.
- Dimitrov, D.S. and Jain, R.K., 1984, Membrane stability, *Biochim. Biophys. Acta* 779:437-468.
- Neumann, E. and Katchalsky, A., 1972, Long-lived conformational changes induced by electric impulses in biopolymers, *Proc. Natl. Acad. Sci. USA* 69:993-997.
- Pohl, H.A., 1978, *Dielectrophoresis*, Cambridge University Press, London.
- Sowers, A.E., 1984, Characterization of electric field-induced fusion in erythrocyte ghost membranes, *J. Cell Biol.* 99:1989-1996.
- Sowers, A.E., 1986, A long-lived fusogenic state is induced in erythrocyte ghosts by electric pulses, *J. Cell Biol.* 102:1358-1362.
- Sowers, A.E., 1987, The long-lived fusogenic state induced in erythrocyte ghosts by electric pulses is not laterally mobile, *Biophys. J.* 52:1015-1020.
- Sowers, A.E.(ed), 1989, in: *Electroporation and electrofusion in cell biology*, Plenum Press, New York, pp. 229-256.
- Stenger, D.A. and Hui, S.W., 1986, Kinetics of ultrastructural changes during electrically induced fusion of human erythrocytes, *J. Membr. Biol.* 93:43-53.
- Teissie, J. and Blangro, C., 1984, Direct experimental evidence of the vectorial character of the interaction between electric pulses and cells in cell electrofusion, *Biochim. Biophys. Acta* 775:446-448.
- Teissie, J. and Tsong, T.Y., 1981, Electric field induced transient pores in phospholipid bilayer vesicles, *Biochemistry* 20:1548-1554.
- Teissie, J., Knuston, V.P., Tsong, T.Y., and Lane, M.D., 1982, Electric pulse-induced fusion in 3T3 cells in monolayer culture, *Science* 216:537-538.
- Tsong, T.Y., 1983, Voltage modulation of membrane permeability and energy utilization in cells, *Biosci. Rep.* 3:487-505.
- Zimmermann, U., 1982, Electric field-mediated fusion and related electrical phenomena., *Biochim. Biophys. Acta* 694:227-277.

WHAT IS MEMBRANE ELECTROFUSION AND WHY DO I STUDY IT?

Arthur E. Sowers (301) 738-0743
Cell Biology Department
Jerome H. Holland Laboratory*
15601 Crabbs Branch Way
Rockville, Maryland 20855

*-owned and operated by the American Red Cross

What is membrane electrofusion?

Membrane electrofusion is an artificial method of inducing membrane fusion which uses an electric field pulse as the fusogen.

Why is membrane fusion important?

Membrane fusion is essential in:

- A. Biological processes (eg. cellular infection by enveloped viruses [including HIV], differentiation, secretion, exocytosis, and reproduction)
- B. Biotechnology processes (eg. genetic engineering, drug delivery, hybridoma production, construct formation, and specialized studies)
- C. Certain fate pathways in interacting lipid systems (vesicles).

While the phenomenon of membrane fusion is highly characterized in many of the above contexts, the mechanism is very poorly understood. While fusogenic agents can be identified whether they be chemical in nature (eg. calcium, polyethylene glycol), a specialized protein (eg. influenza HA spike glycoprotein), a natural protein or peptide used under unnatural conditions, or an energy pulse (electric field, laser light), it is open for argument as to what the definition should be for a fusogen.

- D. There are two additional ways that the study of membrane electrofusion can contribute to membrane biology and biophysics:
 - i) A variety of interacting phenomena, forces, and membrane properties can be probed by an electric pulse as a perturbing force.
 - ii) New biophysical membrane properties and phenomena may be discovered.

How might electrofusion contribution towards understanding membrane fusion?

The use of an electric field pulse as a fusogen has the following unique characteristics:

- A. All fusion events are synchronized
- B. The fusogen is non-chemical
- C. High fusion yields are possible

A second electric field effect, called dielectrophoresis, takes place when a low strength alternating electric field passes through a suspension of membranes and causes them to line up in the so-called pearl chain formation. This results in the membranes coming into contact with each other at two point on each membrane (one point if the membrane is at the end of a chain). The use of dielectrophoresis to induce membrane-membrane contact has the following unique set of characteristics:

- D. The method is mild
- E. The method is non-chemical
- F. The method is completely reversible
- G. The method can cause almost 100 % alignment in only a few seconds.
- H. The method is simple and inexpensive

Items D, E, and F, together with item B above, make it possible to separate from one another the fusogen, the contact of membranes, and the chemistry of the medium. Items G and B (above) make it practicable to study many details of single fusion events if imaging techniques are used.

Essentials of our protocol:

Our experiments utilize ghost membranes from erythrocytes of mammalian species (primarily rabbit and human, but occasionally rat, sheep, dog, cat, cow, horse, and guinea pig). These membranes are arrested in terms of their intermediary metabolism and genetic expression systems, thereby simplifying and controlling their properties. Also, they have: i) a well understood composition, ii) representative components of all cell membranes (i.e. phospholipids, cholesterol, integral proteins, glycocalyx, and cytoskeleton), and iii) are easy to obtain and many protocols have been worked out. They represent an ideal compromise between simple and pure lipid systems such as vesicles and complex systems such as viable nucleated cells. Fusion is measured quantitatively and rigorously by following the movement of a fluorescent lipid analog which is used to label a fraction of all cells, from an original labeled membrane to an originally unlabeled membrane.

Abbreviated chronology of electrofusion with an emphasis on contributions towards understanding the mechanism from our laboratory.

Many early studies of membrane permeabilization by electric pulses (=electroporation= EP) were reported for at least one decade before the discovery of electrofusion (EF). Publications in reviewed journals reporting the discovery of electrofusion and its broad applicability from laboratories of Neumann, Senda, Tsong, and Zimmermann appeared between 1979 and 1980 (Zimmermann claims to be the discoverer based on an abstract published in 1978). The first speculation on the EF mechanism was proposed by Pilwat et al., 1981, and proposed that a fusion intermediate was composed of two concentric pairs of pores (one in each of two close-spaced membranes). Zimmermann's most highly cited review on electrofusion was published in 1982. The appearance of a paper by Neumann et al. (1982) showed that electroporation

could be used for efficient gene transfer, and is also a highly cited paper. Our second EF paper, which characterized EF in the erythrocyte ghost, also stated the discovery of the long-lived fusogenic state and the erythrocyte ghost shape change phenomenon (Sowers, 1984). Use of electrofusion for variety of applications (eg. hybridoma and genetic engineering starts in 1981 - and continues throughout the present with some diminution as newer techniques displace old and use of EF for some applications falls out of favor or new limitations are discovered. More information can be found in the monograph by Neumann, et al. (1989). Reports of asymmetric permeabilization by Rosignol et al. (1983) and Merhle et al (1985) was confirmed in our lab (Sowers & Lieber, 1986), but was found in the opposite hemisphere of the membrane. We found (Sowers, 1986; 1987) that the long-lived fusogenic state was found to be not laterally mobile in plane of membrane. We also found that use of contents mixing indicators as rigorous confirmation for membrane mixing indicators was contaminated by an artifact from electropores but this observation allowed the formulation of the hypothesis for electroosmosis in electropores which also resolved the asymmetric permeabilization discrepancy (Sowers, 1988). Experimental demonstration that fusion event probability can be modulated by biologically relevant changes was shown (Sowers, 1989a) as well as a "averaging" and "dominance" effect when the composition of two membranes to be fused are dissimilar (Sowers, 1989b). Evidence confirming the electroosmosis effect in electropores was recently published (Dimitrov and Sowers, 1990a) as well as our report of initial observation of 0.1 to 4 sec, reproducible, time interval between application of fusogen and earliest observation of evidence for fusion (Dimitrov and Sowers, 1990b, accepted for publication in Biochemistry). A partial analysis of the forces acting on the erythrocyte ghost during dielectrophoresis was also published recently (Dimitrov, et al., 1990). Lastly, we discovered the strong effect of macromolecular solutes on electrofusion yield although its basis is still unclear (Sowers, 1990).

My assessment of the state of our knowledge of the electrofusion mechanism (and its relationship to electroporation) is that much has been learned about the functional relationship between the electric field pulse and both physical parameters and some biological parameters. Further progress in developing mechanisms (or confirming early speculative proposals) will be best aided by additional studies which are aimed at uncovering relationships between functional characterizations and structural correlates.

Related work from other laboratories includes: i) a preliminary study of electropore induction by time-resolved freeze fracture electron microscopy which shows that electropores may have microfunnel ultrastructures (Chang & Reese, 1989), ii) a study of electropore induction in lipid bilayers and cell membranes which shows that the electropores do not reseal quickly (Chernomordik et. al., 1987), and iii) extensive work on both electropore induction and electrofusion in CHO cells in J. Teissie's laboratory at the C.N.R.S. (Toulouse) (eg. Teissie et. al., 1989; Rols, et. al., 1990).

Acknowledgement:

Supported by ONR grant N00014-89-J-1715.

General review paper:

Sowers, A.E. (1989) The Mechanism of Electroporation and Electrofusion in Erythrocyte Membranes, in Electroporation and Electrofusion in Cell Biology, (E. Neumann, A.E. Sowers, and C. Jordan), Plenum Press, New York. 229-256.

Selected papers:

- Chang, D.C., and Reese, T.S. (1989) Biophys. J. 55, 136a.
Chernomordik, L.V., Sukharev, S.I., Popov, S. V., Pastushenko, V.F., Sokirko, A.V., Abidor, I.G., and Chizmadzhev, Y.A. (1987) Biochim. Biophys. Acta 902: 360-
Dimitrov, D.S., and Sowers, A.E. (1990b) Biochemistry. (accepted)
Dimitrov, D.S., and Sowers, A.E. (1990a) Biochim. Biophys. Acta 1022, 381-392.
Dimitrov, D.S., Apostelova, M.A., and Sowers, A.E. (1990) Biochim. Biophys. Acta. 1023, 389-397.
Mehrle, W., Zimmermann, U., and Hampp, R., (1985) FEBS lett. 185: 89-94.
Neumann, E., Schaefer-Ridder, M., Wang, Y., and Hofsneider, P.H. (1982) EMBO J. 1:841-845.
Neumann, E., Sowers, A.E., and Jordan, C.A., eds. (1989) Electroporation and Electrofusion in Cell Biology, Plenum Press, New York 436 pp.
Pilwat, G., Richter, H.-P., and Zimmermann, U. (1981) FEBS lett 133:169-174.
Rols, M.P., Dahhou, F., Mishra, K.P., and Teissie, J. (1990) Biochemistry 29: 2960-2966.
Rosignol, D.P., Decker, G.L., Lennarz, W.J., Tsong, T.Y., and Teissie, J. (1983) Biochim. Biophys. Acta 763: 346-355.
Teissie, J., Rols, M.P., and Blangero, C. (1989) in: Electroporation and Electrofusion in Cell Biology (Neumann, E., Sowers, A.E., and Jordan, C.A., eds.), Plenum Press, 203-214.
Sowers, A.E. (1990) Biochim. Biophys. Acta (in press).
Sowers, A.E. (1989b) Biochim. Biophys. Acta. 985,339-342.
Sowers, A.E. (1989a) Biochim. Biophys. Acta. 985,334-338.
Sowers, A.E. (1988) Biophysical J. 54, 619-626.
Sowers, A.E., (1987) Biophysical Journal 52, 1015-1020.
Sowers, A.E., and Lieber, M.R., (1986) FEBS Letters 205,179-184.
Sowers, A.E. (1986) J. Cell Biol. 102,1358-1362.
Sowers, A.E. (1984) J. Cell Biol, 99, 1989-1996.
Stenger, D.A., and Hui, S.W. (1986) J. Memb. Biol. 93, 43-53.
Zimmermann, U. (1982) Biochim. Biophys. Acta 694: 227-277.

LATERAL PROTON CONDUCTION ALONG LIPID MONOLAYERS
AT THE AIR/WATER INTERFACE

Teissié J.

Centre de Biochimie et de Génétique cellulaires du CNRS
118 Route de Narbonne, 31062 Toulouse, FRANCE
Tel (33) 61335880
Fax (33) 61335886

Experimental evidences have been gathering which suggest that lateral proton conduction may occur along restricted domains in biological membranes. A "microlocalized" pathway would then link the proton pump and the proton sink in a coupling unit and the exchanged proton would not need to be delocalized in the bulk water phase (1).

A direct experimental evidence to the "localized" proton transfer is obtained by a fluorescence assay on lipid monolayers spread at the air/water interface (2). A pH sensitive chromophore covalently bound to the polar group of a phospholipid provided a reliable probe of the proton concentration in the interface region when embedded at a low concentration in the host lipid matrix (3).

Following a pH jump close to the interface, transfer of proton was observed specifically along the interface (2, 4) and the thickness of the proton conductive pathway was estimated by surface potential measurements (5). The transfer occurred along the polar headgroups but only when the film was organized (2). It was modulated by the nature of the polar head groups not as a function of their electrical charge but rather of their size (6). It was observed only in the liquid expanded (LE) state of the film (6). No conduction was detected when the film was compressed to the liquid condensed (LC) and solid condensed (SC) states (6). When present in the subphase, Ca^{++} was suppressing the facilitated conduction along PE monolayers.

Lateral proton conduction was found to occur with monolayers of ether phospholipids of halophilic archeabacteria examined at reduced surface pressure (less than 25 mN/m) on subphases of low (1 mM) and high (4 M) ionic strength (7). Proton conduction was also detected in highly condensed monolayers (pressure larger than 35 mN/m) of the naturally occurring phospholipids (PGP, PG) but was abruptly terminated in tightly packed monolayers of the corresponding deoxy compounds (dPGP, dPG, ddPG) on low ionic content subphases (8). Conduction did occur, however, along monolayers of the deoxy compounds at high surface pressure when spread on a subphase of high ionic strength (4 M). The abrupt termination of conduction upon compression of monolayers of the deoxy compounds on low ionic strength subphases cannot be attributed to any lipid phase transition nor to changes in the lateral fluidity of the monolayers, nor was the pK of the fluorescent interfacial proton indicator affected at high surface pressures. We suggest the occurrence of a conformational change in the polar headgroup region of the deoxy compounds under high compression of the monolayers, but not in that of the naturally occurring phospholipids.

From what is known on proton transfer in solution (9), we proposed that our experimental observations were linked to a network of hydrogen bonds at the level of the polar head groups (6). Any theoretical attempt to describe chemical reactions such as proton transfer at the membrane/water interface must take into account the peculiarities of the system (10). Reduction of dimensions (11, 12), organization of adjacent water molecules (13, 17), electric field inversion (14-16) and hydrogen

bonding should be taken into account when trying to describe proton transfer at the lipid/water interface. At the present stage of our investigations, we suggest that the continuity of the hydrogen bond network between polar headgroups and interfacial water molecules is a request for the occurrence of this conduction. This is strongly supported by the experiments with the deoxy compounds. The most likely change in the polar headgroup of the deoxy compounds would be the formation under high surface pressure of internal hydrogen bonding which would expel water molecules and result in disruption of the conducting network. In the natural phospholipids PGP and PG the presence of the central hydroxyl group would facilitate the formation of stable intramolecular bonding which would render the molecular structure of their headgroups insensitive to high surface pressure and hence preserve the proton conduction network.

As a general conclusion, a precise molecular description of the exchange steps involved in the lateral proton conduction we observed is still lacking at the present stage of investigations. The complexity of the processes favors the experimental approaches as developed in our laboratory and by others (18) which both conclude on repeating hopping of protons along the surface.

(Thanks are due to my coworkers M.Prats, B. Gabriel, A. Lemassu, J.F. Tocanne and to the collaboration with Prof. M. Kates. This work was supported by the CNRS)

References:

- 1- Kell D.B. (1979) Biochim.Biophys.Acta 549, 55
- 2- Teissié J., Prats M., Soucaille P. and Tocanne J.F. (1985) Proc. Natl. Acad. Sci. USA, 82, 3217
- 3- Soucaille P., Prats M. Tocanne J.F. and Teissié J. (1988) Biochim. Biophys. Acta, 939, 289
- 4- Prats M., Tocanne J.F. and Teissié J. (1985) Eur. J. Biochem., 149, 663
- 5- Prats M., Teissié J. and Tocanne J.F. (1986) Nature, 322, 756
- 6- Prats M., Tocanne J.F. and Teissié J. (1987) Eur. J. Biochem., 162, 379
- 7- Teissié J., Prats M., Lemassu A., Stewart L.C. and Kates M. (1990) Biochemistry 29, 59
- 8- Stewart L.C., Kates M. and Smith I.C.P. (1988) Chem. Phys. Lipids, 48, 177
- 9- Onsagers L. (1969) Science, 166, 1359
- 10- Prats M., Tocanne J.F. and Teissié J. (1989) Biochimie, 71, 33
- 11- Abbott E.A. in "Flatland" (1952), Dover Publ., New York
- 12- Chan D.Y.C. and Halle B. (1984) Biophys. J., 46, 387
- 13- Spohr E. and Heinzinger K. (1986) J. Chem. Phys., 84, 2304
- 14- Gruen D.W.R. and Marcelja S. (1983) J. Chem. Soc., Farad. trans. 2, 79, 211
- 15- Hauser H., Pascher I., Pearson R.H. and Sundell S. (1981) Biochim. Biophys. Acta, 650, 21
- 16- Raudino A. and Mauzerall D. (1986) Biophys. J., 50, 441
- 17- Luzar A., S. Svetina and B. Zeks (1984) Bioelectrochem. Bioenerg., 13, 473
- 18- Sakurai and Kawamura (1987) Biochim. Biophys. Acta 907, 705

**Electric Energy Enforced Conformational Oscillations of
Membrane Proteins for Energy and Signal Transductions**

Tian Y. Tsong

**Department of Biochemistry
University of Minnesota College of Biological Sciences
St. Paul, Minnesota 55108**

A protein embedded in a cell membrane is restricted in its motions. It may be allowed to rotate or to wobble around an axis normal to the plane, or to diffuse laterally, but it may not be allowed to flip-flop across the membrane. A chemical reaction catalyzed by such an enzyme is anisotropic or vectorial. An anisotropic chemical system when interacting with a force field that is also a vector quantity may give rise to many interesting effects uncommon to chemistry of a homogeneous phase. Among these is the absorption of energy from a force field by the system and its conversion into other energy forms. A four-state membrane transporter will be used as an example to illustrate how this mechanism can be used to absorb electrical energy and use this energy to pump ions or to synthesize ATP. Among many properties of the field-protein interaction, an applied periodic field is shown to enforce the conformational oscillation of the transporter within its catalytic cycle, thus, enabling the transporter to turn over following a stipulated path. An electroconformational coupling model based on the above concept has been proposed to interpret experimental results of the electric activation of Na,K-ATPase and mitochondrial ATPase. Experimentally, Na,K-ATPase of human erythrocytes has been shown to pump Na^+ , Rb^+ and K^+ up their respective concentration gradients apparently in the absence of ATP consumption. For each pumping activity there are an optimal amplitude and an optimal frequency for the conversion of electric energy into energy of the concentration gradient. Mitochondrial ATPase has also been shown to use electric energy for the synthesis of ATP, in the absence of metabolic sources. These data will be presented and analyzed by the electroconformational coupling model. The same concept has also been extended to construct a piezo-electric coupling model which can convert a pressure or an acoustic signal into the electrochemical potential of an ion.

References

1. Tsong, T.Y. and Astumian, R.D. (1986) Absorption and conversion of electric energy by membrane bound ATPases. *Bioelectrochem. Bioenerg.* 211:457-476.
2. Tsong, T.Y. (1990) Electrical modulation of membrane proteins: Enforced conformational oscillation and biological energy and signal transductions. *Ann. Rev. Biophys. Biophys. Chem.* 19:83-106.
3. Liu, D.-S., Astumian, R.D. and Tsong, T.Y. (1990) Activation of Na^+ and K^+ pumping modes of Na,K-ATPase by an oscillating electric field. *J. Biol. Chem.* 265:7260-7267.
4. Robertson, B. and Astumian, R.D. (1990) Michaelis-Menten Equation for an enzyme in an oscillating electric field. *Biophys. J.* In press.
5. Markin, V.S., Tsong, T.Y., Astumian, R.D. and Robertson, B. (1990) Energy transduction between a concentration gradient and an alternating electric field. *J. Chem. Phys.* In press.
6. Markin, V.S. and Tsong, T.Y. (1990) Mechanoelectrical transduction of energy and signals: A piezo-conformational coupling model. Submitted for publication.

ALAMETHICIN - A VOLTAGE DEPENDENT ION CHANNEL

Igor Vodyanoy, University of California, Irvine CA; Office of Naval Research, Arlington VA. USA

Alamethicin is a small channel-forming peptide only 20 amino acids long it is thus simple to modify it in ways which alter its function more or less predictably. The crystal structure of alamethicin is known, and its properties and conformation in organic non-polar solvents have been extensively investigated. These results indicate that alamethicin has a stable alpha-helical conformation of about ten residues long beginning at the N terminus and at least in some solvent systems, a region of beta-sheet at the C-terminus.

Alamethicin induces a very voltage-dependent conductance in planar bilayers and in the membranes of some living cells. Because several alamethicin monomers must aggregate together to form a channel, its study provides direct information about the forces which hold channels together.

ALAMETHICIN ADSORPTION

a. Kinetics

One difficulty in the study of alamethicin as a model for formation of channels in biological membranes has been obtaining information about the non-conducting state. We know how many channels form at a given voltage for a given aqueous concentration of alamethicin, but we do not have a very good idea of how many alamethicin molecules are adsorbed to the planar bilayer or of the physical state of the adsorbed molecules. Recent studies of alamethicin interaction with lipid vesicles using circular dichroism support the notion that alamethicin incorporates into the lipid phase to a significant extent.

Rizzo, Stankowski and Schwarz using a general thermodynamic approach, have shown theoretically that the concentration dependence of the alamethicin-induced conductance could be explained by a voltage-dependent adsorption and aggregation of alamethicin mediated by interaction of the alamethicin dipole and an applied electrical field. Thus it is very important to understand how alamethicin adsorbs to the lipid bilayer.

We were able to study the voltage dependent alamethicin adsorption experimentally. We have shown that alamethicin monomers interact with each other being adsorbed and that interaction is strong even at the small applied voltages.

If we assume that alamethicin conduction is due to an ionic channel consisting of aggregated alamethicin n-mer then such kinetics are consistent with the idea that aggregation of alamethicin molecules proceeds as a bimolecular reaction.

The course of aggregation with time is determined by two factors, the Brownian motion and by the molecules interaction when they come close together. If we assume that molecules form a permanent contact at the first encounter then the problem will be identical to the so called 'rapid coagulation'. The rate of such aggregation was analyzed by Von Smoluchowski.

Our results show that the alamethicin-induced transmembrane current increases to its maximum value in about 3-6 minutes after alamethicin addition and then declines to a steady-state value over the next 25-30 minutes. We suggest that the alamethicin molecules aggregate first into dimers and after a certain time additional monomers collide with these multimers. The multimers also collide amongst themselves. Thus the surface concentration of the conducting species appears to increase with time to a maximum and decrease toward its equilibrium value. The steep rising phase can be attributed to rapid formation of the n-mer conducting species, and the falling phase is due to the diminution of the concentration of this species as more and more alamethicin monomers becomes incorporated in higher than n order non conducting aggregates.

b. Pseudocapacitance

Alamethicin and its derivatives modulate the voltage-dependent capacitance at voltages lower than the voltage at which alamethicin-induced conductance is detected. The magnitude and sign of this alamethicin-induced capacitance change depends on the aqueous alamethicin concentration and the kind of alamethicin used.

Our experimental data can be interpreted as a potential-dependent pseudo-capacitance associated with adsorbed alamethicin. Pseudo-capacitance is expressed as a function of alamethicin charge, its concentration in the bathing solution and the applied electric field. The theory describes the dependence of the capacitance on applied voltage and alamethicin concentration. When alamethicin is neutral the theory predicts no change of the voltage-dependent capacitance with either sign of applied voltage. Experimental data are consistent with the model in which alamethicin molecules interact with each other while being adsorbed to the membrane surface. The energy of this interaction depends on the alamethicin concentration.

ALAMETHICIN TETRAMER CONDUCTANCE

An alamethicin pore was designed with an amide backbone mouth at the C-terminus. The actual peptide is a tetramer of alamethicin 1-17 in which four monomers have been attached to a tetramer of lysine through the epsilon amino groups. Our preliminary data show that this peptide, which we refer to as Ac-(Lys(Alamethicin 1-17))₄-NH₂, after addition to the phosphatidylethanolamine bilayer, causes voltage-dependent conductance with a reduction of concentration dependence and a current-voltage curve steepness of about 5 mV per e-fold of the current. The conductance is expressed as channels of the basic unitary conductance (about 2.5 nS). These data are in accord with our channel model in which voltage-dependence is explained by interaction of the electric field with the dipole moment of the alpha helical part of alamethicin.

Acknowledgement

This work is supported by the Office of Naval Research.

Conformational Dynamics of a Transmembrane Channel

Watt W. Webb, Lorinda Opsahl and Don-on Dan Mak

Applied Physics, Cornell University

Ithaca, New York 14853

607-255-3331; FAX 607-255-7658

The alamethacin channel now provides an attractive experimental system to observe the dynamics of fluctuations and conformational changes of membrane proteins through several synergistic experimental approaches based on high resolution single channel electrical recording of the channel conductance. We are measuring conductance state switching probabilities and kinetics and their multiple correlations and the conductance fluctuations in each open conductance level. These properties are being measured as a function of key environmental parameters: membrane potential, lipid composition with respect to head group size and charge, curvature propensity and hydrocarbon chain length, aqueous phase ionic strength, viscosity and hydration chemical potential, and (perhaps most important) membrane tension. In addition certain site specific mutations of the alamethacin monomer molecule are being introduced by protein engineering techniques to test our understanding of channel structure.

These experiments have revealed three unusual phenomena which are currently being measured systematically to gain understanding of the molecular dynamics of this channel protein:

1) The conductance noise spectra of the channel during its residence time in each open state is being measured systematically and found to exceed the intrinsic ion shot noise by several orders of magnitude at low frequencies and to extend smoothly, at nearly constant in power spectral density, to our measurement limits around 40 kHz. We tentatively attribute this noise to conformational fluctuations of the channel protein assembly and are currently carrying out diagnostic experiments to test this idea. The original strategy underlying this program on alamethacin was to measure such conductance fluctuations in order to probe the low frequency cooperative vibrational modes of membrane proteins in order to identify the "soft" modes that must exist to accommodate the changes of conformation state that underlie ion current switching. That strategy appears to be working.

2) The dependence of state switching on membrane tension has been measured to determine that the alamethacin channel is strongly stretch sensitive. This stretch sensitivity is a common property of many cell membranes and is believed to provide the fundamental mechanism of mechano-electrical transduction that underlies hearing and sensation of six components of acceleration. Membrane tension is induced by applying a controlled transmembrane pressure and is measured by monitoring membrane curvature. The stretch sensitivity found in alamethacin reconstituted into pure lipid membranes is highly reproducible, unlike

most cell membrane stretch sensitivity, and appears to be attributable to a mechanical work term in the relative free energies of the channel states.

3) Measurements of the conductance state occupation probabilities and switching dynamics, incidental to the above two directed projects, have been analyzed by Stefan Brundobler. His analysis revealed anomalous dynamics including a non-exponential distribution of the residence times and an apparent history-dependence of the probability distribution of the residence times of the various states. The most interesting result can be described by naming the distinguishable conductance levels 0, 1, 2, 3, 4, . . . n in order of increasing conductance; then we find that the up switching events, say n to n+1, are distinguished from the down events, say n to n-1, and that the residence times in various levels depend on both the class of event by which the system departed the level (as is generally true) and by which the system entered the level (as would be true if the system remembered its previously occupied level). Thus conditional dynamics differ for pairs of transition like (1, 2, 1), (3, 4, 3) from those like (3, 2, 1) and (5, 4, 3), and those like (2, 1, 2) and (4, 3, 4). This sort of result implies non-Markovian processes, that is, a system that has a memory and violates the principle of microscopic reversibility, a concept whose application to channels excites continuing controversy. On the other hand, we can account for our results as a conventional Markov process if we invoke the idea that each conductance level may really consist of several different states of indistinguishable conductance but different free energy. In the sense of statistical thermodynamics, these are non-degenerate states that are not distinguished by the conductance.

These experiments suggest some interesting concepts about channel molecule structure and its relation to channel function.

**NEW APPROACHES, MECHANISMS, APPLICATIONS AND COMPARISON OF DNA
ELECTROTRANSFECTION WITH BIOLISTIC TECHNOLOGY.** Alexander V. Zelenin,
Engelhardt Institute of Molecular Biology, USSR Academy of Sciences, Vavilov
Street 32, Moscow 117984.

Research interests and possible topics of my presentation:

1. New approaches to cell electrofusion
 - A. Electrofusion of cells growing on conductive film
 - B. Electrofusion of cells in the course of centrifugation
2. Cellular and membrane mechanisms of cell electrofusion
3. Applications of cell electrofusion
 - A. Hybridoma production
 - B. Obtaining of hamster x human cell hybrids
 - C. Regulation of DNA synthesis in heterokaryons obtained by electrofusion.
4. Introduction of foreign genetic material into animal cells by high velocity mechanical DNA injection (biolistic technology); comparison with other methods including electrotransfection.